Subsurface Mapping of the Early-Middle Miocene Retrench Sandstones along the La Fortune Anticline, Oropouche Oil Field, Southern Basin, Trinidad, W.I.*

Stefon Harrypersad[1], Xavier Moonan[2], Victor Young On[2], Shiraz Rajab[2], Fawwaaz Hosein[2], Ashleigh Costelloe[2], and Brent Wilson[2]

Search and Discovery Article #20372 (2016)**
Posted October 31, 2016

*Adapted from extended abstract based on oral presentation given at AAPG/SEG International Conference & Exhibition, Cancun, Mexico, September 6-9, 2016

[1]Department of Geography & Geology, University of the West Indies, Mona Campus, Jamaica (stefonharrypersad2916@gmail.com)
[2]API Petroleum Company Limited, 51A Siparia Old Road, Fyzabad, Trinidad

Abstract

The Early Miocene Retrench Sandstone turbidites are found encased within the heavily folded deep-water Golconda Marls of the Cipero Formation within the Southern Basin of Trinidad. These sandstones serve as the primary reservoir for the onshore Oropouche Oil Field along the west south-westerly plunging, south-easterly verging detached La Fortune Anticline. During the Early-Middle Miocene, the apparent eastward migration of the leading edge of the Caribbean Plate resulted in an oblique collision with the attenuated northern margin of South America continental crust, generating foredeep settings in the Southern Basin of Trinidad, into which the Early Miocene Retrench sand turbidites were deposited in tectonically related pulses within synclinal lows. Continued transpression into the Pleistocene resulted in the sands being incorporated within the Present Day heavily imbricated and tear fault dissected La Fortune Anticline.

From 1955 to 2015 a total of one hundred and fifteen wells have drilled and tested the prolific Retrench sandstones along the La Fortune Anticline, yet very little scientific evaluation of these reservoirs have been undertaken. In May 2015, the current operator, API Petroleum, embarked on a three well drilling campaign, including both development and semi-appraisal wells, namely AO-116, AO-117 and AO-118. Realizing the increase in step-out well challenges, a first-of-its-kind integrated subsurface mapping of the Retrench reservoirs was undertaken to better understand the properties of the reservoirs and to de-risk future appraisal drilling. The subsurface evaluation workflow integrated petrophysical correlation of vintage electric logs, operations and drilling data, as well as paleontological reports. Interpretation along semi-regional 2D and 3D seismic datasets allowed for the generation of structure, net sand and net oil sand maps.

Rock cuttings from the recent drilling campaign were used to generate thin sections to evaluate the texture, mineralogy and depositional environment of the primary reservoir. Thin section analysis was also undertaken on recent Retrench sand outcrops near the village of Golconda, some five kilometres north east of the Oropouche Oil Field. Detailed biostratigraphic analysis of the rock cuttings were undertaken to relate the benthic to planktonic foraminiferal assemblages in an attempt to assess the water depth and the depositional environment.

Finally, structural restorations along seismic cross sections were undertaken to simulate the evolving bathymetry of the Early-Middle Miocene foredeep for each of the Retrench reservoirs, aiding in the prediction of the turbidite fairway and de-risking future drilling prospects within the Oropouche Oil Field, La Fortune Anticline.

Introduction

The Early Miocene Retrench Sandstone has been interpreted as a deep-water sandy turbidite deposit which serves as the primary reservoir for the Oropouche Oil Field in southern Trinidad (Figure 1b). This sandstone produces both oil and gas from penetrations as shallow as 9 m (29.5 feet) to as deep as 1.5 km (4,921 feet) below mean sea level. The Oropouche Oil Field trends WSW-ENE, encompassing an area approximately 8 km long by 3 km wide and has been in development since 1956 with a total of 118 wells drilled to date. As such, much of the field remains largely underdeveloped. The field is located on the onshore southern sub-basin of Trinidad, approximately 4 km south the city of San-Fernando within the Oropouche Lagoon. The field is developed on the plunging WSW-ENE trending, southeast verging compressional La Fortune Anticline. These anticlines are prominently dissected by a series of generally N-S trending tear faults which dislocates the anticlinal axis, creating a series of complex structural traps. These structural features, together with a very strong stratigraphic component involving pinchouts and rapid changes in sand thickness significantly influences the size and geometry of reservoirs within the Oil Field.

The Retrench Sandstone Member of the Cipero Formation is divided into three zones (lower, middle and upper units) based primarily on biostratigraphy, the uppermost of which is termed the Golconda Marl. The lithology of the Cipero comprises grey banded calcareous clays (Wilson and Hayek, 2015). Within the brown coloured facies of the Cipero Formation, there occurs a fine-grained sandstone titled the Retrench Member. These sandstone units can be reminiscent of the Late Oligo-Miocene Nariva Sandstones (Kugler, 2001; Farfan and Wilson, 2015). The upper and middle units which are of Early Miocene age, comprise the Golconda Marl and Retrench Members, respectively. According to Persad (2011), this Retrench turbidite material was deposited in a series of west-southwest to east-northeast foreland uplifts and foredeep basins, formed from the late Oligocene to early Miocene. These are recognised as a series of submarine fan fairways, which host oil and gas fields. They include the newly discovered Oligocene Naricual fairway, the Lower Miocene Brasso, Nariva, Retrench and Herrera fairways and other younger reservoir trends to the south/southeast. This is the primary reason why the Retrench Member is characterised by numerous pebble beds, slump masses of Eocene material and shallow-water limestones, in contrast to the characteristically open water Cipero sediments (Wilson and Hayek, 2015).

Cipero Formation

Cushman and Stainforth (1945) divided the Cipero (marl) Formation (Figure 1a) into three planktonic foraminiferal zones: lower (*Globigerina concinna* zone), middle (*Globigerinatella insueta* zone) and upper (*Globorotalia fohsi* zone). Bolli (1947) divided the Cipero Formation into 11 biozones and subsequent taxonomoic work by Bolli (1957) provided the framework for low-latitude planktonic foraminiferal biostratigraphy of the Neogene. Paleoenvironmental interpretations based on planktonic foraminifers, by Cushman and Stainforth (1945), suggested the influence of warm water currents (based on *Globigerina*) and water depths of ≥ 55 m (based on the lack of *Archaias* and related species). Benthonic specimens of *Lagena*, *Nodosaria* and Ellipsoidinidae suggested depths between ~ 91 m and 183 m. Stainforth (1948) revised the paleoocean depths to 400-500 m, describing the Cipero marl as an open water *Globigerina* ooze, which should be divided into lower (Paradise) and upper

(Cacatro) members. More recent reconstructions of the Oligo-Miocene paleo water-depth, based on extant foraminifers in the Cipero Formation, argue for deeper waters of 1500-3000 m (Farfan and Wilson, 2015). The paleobathymetry of the southern basin, at the time of the Cipero deposition, might be clarified using the relative abundance of planktonic specimens (Wilson 2003, 2005), although in deep water this statistic is influenced by dissolution also (Nguyen and Speijer, 2014).

Oxygen and carbon stable isotope measurements of planktonic foraminiferal shells recovered from the Cipero Formation (latest Oligocene to earliest Miocene), confirm an oligotrophic open-ocean setting, with a well-defined and seasonally stable thermocline separating surface waters of 27 ºC and sub-surface waters of 13 ºC (Pearson and Wade, 2009). Three planktonic foraminiferal assemblages characterized the upper, mixed and deep thermocline layers. Wilson (2008b) defined three abundance biozones for the Cipero Formation (exposed at Cross Crossing, central Trinidad), using benthonic specimens of foraminifers and a bottom-up approach to SHE analysis for biozone identification (SHEBI). Prior to Wilson's (2008b) zonations, the majority of analyses of the Cipero Formation were based on the more abundant planktonic foraminifers. Further examination of the benthonic foraminifers would supplement existing depositional models for the Cipero Formation. Using the assemblage turnover index (ATI) would be an alternative approach to assigning biozones, based on peak assemblage turnovers in the benthonic foraminiferal species.

Methods and Material

Submarine reservoir fairways of the Lower Miocene Brasso, Nariva, Retrench and Herrera are still under-explored (Persad, 2011). Available data are quite fragmented or absent. This research is aimed at examining the Retrench Sandstones through a multi-disciplinary analysis of lithology, biostratigraphy, depositional environment, structural physiognomies, seismic interpretations, and evolutionary characteristics in refining the current understanding of the area's geological evolution. This involved time consuming data collection and material preparation in ensuring that findings were a true reflection of the paradigms being investigated.

Structural Restorations and Geophysics

Structure and geophysical investigations represented a core component of this multi-disciplinary research and required a significant amount of effort. Data collection commenced through a formal internship with API Petroleum Company Limited on July 1, 2015 at their Oropouche farm-out sub-office located on the La Fortune Pluck Road Woodland and continued until August 28th, 2015. The company provided all the necessary well files, well logs, biostratigraphic reports, updated production data and seismic cross sections required.

The first challenge involved creating cross sections from available strip logs in the designated study area. This allowed for the mapping of four prominent sandstone packages, the SH1 (AO8), SH2 (A015), SH3 (AO 10), and SH4 (AO22) sands throughout the designated study area. Five strip-log cross sections were created, the first of which was a cross-section along the southern flank, parallel to the axis of the AO4 Anticline trending WSW-ENE through wells AO29, AO21, AO15, AO12, and AO26. Another four were done orthogonal to strike or demonstrating the dip of anticline along the following wells:

- AO31- AO103- AO16- AO29
- AO102- AO8- AO17- AO21
- AO93- AO19- AO83- AO12
- AO26- AO106- AO101- A024

These cross sections allowed for the internal structure of the anticline to be mapped using biostratigraphy reports and sand signatures which allowed for common trends and anomalies to be detected. Quantitative data collection for each of the four mapped sand packages (SH1, SH2, SH3 and SH4) involved recording sand top readings, gross and net sand thickness values, net pay values, production data, well-bore angles, azimuth dips, water contacts, pressure (PSI) values in reservoirs and porosity readings. This dataset was used to generate structure contour maps, sand thickness contour maps and net pay contour maps for each of the four sands. Pressure readings, production data and water contacts were used to determine appropriate faulting regimes, water contacts and lowest known oil. Well bore dips and calculated formation dips were used to correct apparent thickness into true thickness. These were done to ensure that interpretations were based on as accurate data as permitted.

Likewise, seismic cross-sections generated by API's geophysics consultant Mr. Victor Young-On, along the same five cross section zones were provided. These cross sections were used to correlate with strip-log cross sections and to perform structural restorations and paleobathymetry reconfiguration in unravelling the evolution of this anticline and its depositional regimes. This was achieved through the use of geophysical software PETREL, for modeling of the data sets acquired. Restoration concepts put forward by Moonan (2011), were applied where known surfaces such as the sand tops and true stratigraphic thicknesses were used in an attempt to restore sea floor bathymetry during specific times of deposition and to create structure maps and sand maps. This was achieved by loading into Petrel, all UTM well-locations for study area, rotary table elevations, well-bore angles, all the sand top picks, sand thicknesses, net pays and 2D and 3D seismic cross-section sand top picks. This allowed for structure maps and sand thickness maps to be contoured using a different contouring technique as compared to those done manually for the SH1, SH2, SH3 and SH4 sandstones. The paleobathymetric restoration was achieved by using two successive sand tops (SH1-SH2, SH2-SH3 and SH3-SH4) in acquiring the true stratigraphic thicknesses for the entire study area, and with the assumption that thicker (thinner) units are associated with paleobathymetric lows (highs), these stratigraphic thicknesses obtained were then multiplied by -1 to invert the values, such that 0 represents the unfolded top of the overlying sand body. The inverted values were then contoured by PETREL to obtain the three paleobathymetric maps which represented the depositional surface at the time the SH2, SH3 and SH4 turbidites were deposited. Net sand maps were draped over these paleobathymetric maps in observing common trends.

Field assessment of the OAS Quarry along the M2 Ring Road Woodland provided a fantastic opportunity to understand faulting regimes and depositional paradigms in an exposed analogue. Pictures and measurements were taken and used to illustrate the complex faulting occurring in the area. Likewise, the sandstone and marlstone outcrops at the Golconda Interchange provided another unique opportunity, to experience at the surface, paradigms that were occurring at even up to -1280 m (-4200 ft) such as faulting, pitchouts and folding. Samples acquired at this outcrop were used in creating thin sections and sample dating using biostratigraphy. These helped to shed light on the complex deformation of the area and aided invaluably in understanding the structural history and evolution of the area, along with reservoir properties and provenance of these sandstones.

Paleontology

For this article, paleontology was done to understand the paleoecology and biostratigraphy of the Retrench Sandstones drill cuttings. Approximately 10 g of each 9.15 m (30 feet) interval, were soaked in water and sodium bicarbonate and gently heated for about 20 minutes until disintegrated, then gently washed using a 63 μm sieve to remove silt and clay detritus and dried on a low heat (Wilson and Hayek, 2015). This was done for twenty-eight samples between interval -90 m (-295 feet) and -450 m (-1476 feet) for the AO 117 well drilled in the Oropouche Oil Field. From the dried residue of each sample, the first 200 benthonic and planktonic specimens were picked and placed on separate slides, the numbers of each recorded for the planktonic to benthonic ratio. Further, benthonic specimens were picked to achieve a total of 200 benthonic specimens for statistical analysis. Not all planktonic specimens need be identified, but only those index fossils that provide the narrowest age range for each sample, using Bolli and Saunders' (1985) Oligocene to Holocene low latitude planktonic foraminifer zones. Identification of the benthonic specimens followed the taxonomy of Cushman and Stainforth (1945) and Bolli, Beckmann and Saunders (1994).

The objectives of this paleontology aspect were to:

1) Provide a paleoenvironmental interpretation of the Retrench sandstones using benthonic foraminifer species characteristics such as diversity and dominance.
2) Assess possible sea level changes during deposition using *Amphistegina* sp. to benthonic ratios for 28 samples and marker species.
3) Identify changes in major versus minor dissolution in *Amphistegina* sp., population for the 28 benthonic samples in determining trends associated with deposition.
4) Incorporate findings into paleogeographic depositional model and for comparison with lithological log and gamma ray log for A0117 up to a depth of -450 m (1,476 feet).

Sedimentology

The sedimentological aspect of this research involved the use of drill cutting donated by API Petroleum Company Limited from their 2015 drilling campaign (AO116, AO117 and AO118) in the Oropouche Oil Field. These samples were utilised to create lithological logs which ranged from -230 m for well AO116, from surface to -1275 m for well AO117 and from -490 m to -1160 m for well A0118. For each interval, grain size measurements, sorting, grain shape, colour, mineral composition, organic content, sand concentration and other noteworthy paradigms were recorded. These were then sequentially recorded on lithologs for each well and then used to identify sequential similarities and differences from surface to terminal drill depth. Noteworthy trends were carefully correlated with radioactivity and resistivity logs in determining sampling accuracy and consistency.

Petrology

The clast lithologies of the Retrench sandstones was accessed through the use of thin sections which were created at the Department of Geography and Geology, UWI Mona, Jamaica. Five samples across all three wells (AO116, AO117, 10118), an outcrop sample collected from

the Golconda Interchange exposure and a sample from the Point-a-Pierre Formation to test for provenance were used to create thin sections. The recorded depth for the thin section Oropouche well samples were as follows:

AO116: -145 to -156 m (-475 to -511 ft)
AO117: -322 to -332 m (-1056 to -1089 ft)
AO117: -500 m (±5 m) (-1640 ft ±16 ft)
AO118: -823.50 to -835.50 m (-2700 to -2741 ft)
AO117: -1220 to -1239 m (-4000 to -4065 ft)

In creating the thin sections, five carefully observed steps as outlined by Green in (Steele 2014) were diligently followed in ensuring that the final product met the necessary standards. For each section, grain size, sorting, shape, colour, mineral composition, organic content, sand concentration, fracturing, monocrystalline versus polycrystalline quartz and other noteworthy characteristics were recorded. Point counting for five well samples and Golconda Interchange outcrop was done in classifying rocks using Pettijohn's QFL scheme for arenites. This allowed for invaluable well and outcrop comparisons from surface down to -4200 ft. Point counting and comparisons allowed for provenance of material to be assessed in determining depositional history and evolution of the basin.

Results

Paleontology

From the Retrench sandstones of the Oropouche Oil Field well samples, the presence of planktonic index species *Globorotalia scitula scitula* and *Globorotalia mayeri* was used in age dating the samples, the deepest and shallowest sampled depths of -434 m (-1424 ft.) to -446 m (-1463 ft.) and -91 m (-289 ft.) to -100 m (-328 ft.) for well AO117, respectively, were dated to be N9-N14 of the early middle Miocene. The presence of the index species *Globorotalia foshi peripheroacuta* (Figure 2a) *and Globorotalia foshi peripheroranda* however, narrowed this age of deposition to N9-N10 of the early Middle Miocene as seen in Figure 2. This is against existing well-file reports which state that the Retrench sandstones are Early Miocene (N7) turbidites. These results suggest that the Retrench sandstones of the Oropouche wells are Early-Middle Miocene in age (N9-N10).

The depositional environment of these sandstones was inferred through the benthonic assemblages, specifically one genus and three species which were identified, and their populations were tabulated for each of the 28 samples. Barker et al. (2009) described the genus *Amphistegina* sp. genus (Figure 2b) as a middle neritic, fore-reef specimen and Hallock (1981b) suggested that based on experimental growth of *Amphistegina*, a relationship between growth and optimum light conditions was observed, with those living in the dark growing very slowly. This is with the exception of the lower limit of the Mediterranean species *Amphistegina lessonnii* which is controlled not by light, but by the thermocline at water depths of 60-70 m. Wilson (2004) also observed *Amphisteginas* in the Brasso Formation of the Central Range and in fore-reef areas of St. Lucia in modern deposits (as cited in Wilson, 2011). Moreover, Hallock (2000) suggested that the living conditions, environment and ecology of *Amphistegina* resembles a "coral reef ecology" and environment but goes further to suggest that there would be an increase in *Amphistegina* where these is a decline in coral cover with suitable water quality maintained. Lutze and Thiel (1989) indicated that

Planulina wuellerstorfi (Figure 2c) is an epifaunal species, which prefers a living position just above the sediment-water interface which enhances its chances of feeding in slow streaming water. These foraminifers attach themselves to sponge skeletons, stones and other objects protruding out of the substrate and live in lower bathyal depths around 1500 m depth. Further, *Uvigerina paravula* (Figure 2d) is common at depths above 300 m and rare below 400 m (Denne and Gupta. 1988) and is associated with less turbid conditions as compared to middle neritic Amphistegina. *Cibicidoides crebbsi* occurs at of lower bathyal depths (-1000 m) in the Gulf-of-Mexico and *Cibicidoides pachyderma* thrives as an upper bathyal foraminifer and is frequently transported down slope thereby occurring at different locations. Both *C. crebbsi* and *C. pachyderma* are associated with relatively stable, well-oxygenated, low-energy conditions related to a good supply of organic matter (Kender et al., 2009).

The abundance of *Amphistegina* fluctuated from the deepest sample to the shallowest sampled depth as seen in Figure 3. There is an increase in *Amphistegina* sp. abundance between depths -313 m (-1027 ft.) to -322.50 m (1058 ft.) and depths 341.5 m to 352.50 m which is above the mean plus standard deviation baseline used as an estimation of normal conditions. Both C. *Crebbsi, C. pachyderma and Planulina wuellerstorfi* are all still prominently present throughout the 28 sampled intervals which indicated that *Amphistegina* sp. is an allochthonous element being brought into the middle-lower bathyal basin. Above depths -313 m (-1120 ft.) to -322.50 m (-1152 ft.), conditions immediately summersault into below normal conditions with only a few spikes in *Amphistegina* sp. population. These spikes still occurred significantly below the mean plus standard deviation baseline used as a marker for average conditions.

The *Amphistegina* sp. to planktonic ratio (Figure 4) is another robust indication that the allogenic shallow water *Amphistegina* sp. has been transported into >1500 m deep basin depocentre. The graphs shows an almost identical overprint of what is being observed in the benthonic abundance graph as seen in Figure 3. There is a gradual increase in the ratio from the deepest sampled depth to sampled interval -313 m (-1027 ft.) to -322.50 m (1058 ft) which strongly hints to a transgressive system with shallow water facies and foraminifers being transported over the shelf edge into the deeper middle-lower bathyal basin floor as turbidite fans. Above this sampled depth, a sudden tumble to below normal conditions is again observed.

The preservation of *Amphistegina* sp. major versus minor dissolution graph (Figure 5) indicated another very interesting trend with a lower proportion of dissolution being associated influx of these genus into deeper waters as seen between the deepest sampled depth to sampled interval -313 m (-1027 ft) to -322.50 m (1058 ft). A higher proportion of dissolution is seen when there is a lower influx of *Amphistegina* sp. into the basin above sampled interval -313 m (-1027 ft) to -322.50 m.

Lithology

The lithologs revealed that grain sizes deviated between very fine upper (0.088 - 0.125 mm) and medium lower sands (0.25 - 0.35 mm) with the majority of samples occurring as fine lower sands (00125 - 0.177 mm) as seen in Figure 6. This was seen quite prominently in the lithologs for AO117 and AO116. Throughout the samples, sorting remained good with angular grains existing constantly. Chert grains accounted for 10% to as much as 30% of the samples and occurred as black and brown grains. The dominant mineral was quartz accounting for 60-85% of the samples. All the samples fizzed profusely with the application of dilute hydrochloric acid due to the presence of calcareous marls and significant amounts of foraminifers, especially planktonics. Oil sand packages were observed to be associated with larger grain sizes, greater

sand grain concentrations or on most instances, both. Thicker sand packages up to 35 m occurred deeper in the wells as seen in AO117 and progressively decreased in size further up the logs. Smaller, more frequent sand packages between 1 to 12 m in sizes, with closer spaced intervals between them occurred further up the log. AO116 showed more fluctuations than AO117 possibly due to inadequate sampling techniques applied during drilling.

Petrology

Texturally, the five thin sections created for the Oropouche wells Retrench Sandstones demonstrated little deviance in grain size with sample AO117: -1220 to -1239 metres (-4000 to -4065 ft) occurring as a fine upper sand (0.177-0.250 mm) and the other four well samples AO116: -145 to -156 metres, (-475 to -511 ft), AO117: -322 to -332 metres (-1056 to -1089 ft), AO117: -500 m (±5 m) (-1640 ft ±16 ft) and AO118: -823.50 to -834.50 metres (-2700 ft - 2742 ft) , all occurring as fine lower sands (0.125-177 mm). All five samples were well-sorted with all exhibiting very angular grain boundaries. The dominant minerals represented in the sections were quartz, chert, calcite grains, and intensely weathered feldspars. Significant amounts of foraminifers, especially planktonic foraminifers were observed in all the sections with tests made of calcite. A very minor amount of pyritized grains and forams were observed in some samples. The mineral composition based on 300 grain point counting indicated that all the well samples and the Golconda Interchange outcrop were sub-lithic arenites based on the Pettijohn's QAF classification scheme for arenites as seen in Figure 7.

Quartz is the most dominant mineral in occurring in the five sections as seen in the Pettijohn's QFL triangle (Figure 7) and thin sections (Figures 8-9, 10-11 and 12). Anhedral grain edges dominated the all five sections with good sorting being observed throughout. Prominent alteration haloes caused by pressure solutions or dissolution of grain edges, fluid inclusions and recrystallization into open fabrics were prominently observed in all sections also. Concavo-convex, sutured grain boundaries and intensely fractured interiors are quite evident in all the Oropouche thin sections, increasing quite conspicuously from the deepest well to the shallowest, with the most deformed quartz grains occurring in section AO117: -322 to -332 m and AO116: -145 to -156 m. This significant quartz deformation appears to have contributed positively to porosity. The quartz grains are significantly more deformed than the cherts, feldspars, calcite and foraminifers. Monocrystalline quartz is dominant with a few severely deformed grains which appeared to display polycrystalline tendencies as non-uniform, shadowy extinction, sutured grain boundaries, grain boundary migration and grain flattening fabrics.

Altered feldspars accounted for a minor proportion of the five well samples, and were somewhat difficult to identify because of intense weathering of grains. These grains displayed 2 directions of cleavage at right angle, straight extinction, low interference colours and low relief which is characteristic of potassium feldspars. The weathering of grains disguised twinning but this was nonetheless observed in a few distorted grains. These grains were quite fractured internally and at boundaries.

Well-formed calcite crystals accounted for up to 30% of AO117: -1220 to -1239 m (Figure 8) and up to 40% of AO118: -823.50 to -834.50 m (Figure 9), with less than 1% being observed in the overlying three sections. These calcite grains were well formed with the majority occurring as lenticular crystals with subhedral grain boundaries and moderate relief in PPL. Moderate grain fracturing was observed. Some dolomites were inferred based on the presence of twin lamellae not aligned parallel to cleavage planes.

Lithic fragments (chert) increased in concentration from the deepest sample AO117: -1220 to -1239 m 12.6% to 20.6% for the shallowest sample AO116: -145 to -156 m and displayed grain sizes all less than 0.4 mm. These grains displayed anhedral boundaries, were conspicuously black or brown in PPL, and showed no evidence of cleavage or twinning in PPL or XPL. This cryptocrystalline mineral exhibited very little deformation and boundaries and grain interiors were vastly better preserved than all other mineral constituents of the five sections.

Golconda Interchange Retrench Sandstone outcrop (GIRSO) (Figure 13), unlike the well samples was not washed and was impregnated with a blue dye which gave an indication of porosity. This sandstone was classified as a lithic arenite as seen in Figure 7 with very fine upper sand (0.088-0.125 mm) which exhibited angular grain boundaries. The grains were well sorted and the minerals observed were quartz, lithics (chert) and very minor feldspars. The major distinction between the GIRSO and well samples was the quartz grains observed in the GIRSO, was in no way as fractured as those observed in the well samples and the majority of quartz grains did not exhibit pressure solutions, grain boundary migration, recrystallization and internal deformation. The majority of the quartz were monocrystalline and no evidence of polycrystalline grains were observed. The cement observed in this thin section was a clayey calcareous marl which exhibited light brownish green colours in PPL and high order pinkish brown interference colours in XPL which reiterates it's a calcium carbonate mud.

The Point-a-Pierre Formation sandstone, used to test for provenance for the Retrench sandstones, was classified as a quartz arenite and existed as a very coarse lower sand (1.0-1.41 mm) which was moderately sorted with anhedral grain boundaries. The grains displayed white to grey colours, low relief, low refractive index and absence of cleavage or twinning in plane polarised light. Quartz crystals were internally fractured with concavo-convex sutures, pressure solutions, undulose extinction and recrystallization within grain structures all being observed in XPL. Smaller quartz grains also coalesced to form larger grains through grain boundary migration and nucleation of small grains. This sandstone is tightly packed and grain boundary migration was quite evidently observed with a few extremely thread like (0.02 mm) lenticular calcite grains being coalesced with quartz grains thereby preventing deeper grain boundary migration. The majority of the quartz were monocrystalline with just a few grains occurring as polycrystalline quartz with shadowy extinction, sutured grain boundaries and grain flattened fabrics. This sandstone also ranged from fine grained to very coarse grained (Figures 14a, b and c) which also host hydrocarbons as seen in oil impregnated section Figure 14c.

The Cunapo conglomerate (Figure 15) was another potential provenance source of the cherts deposited in the Retrench fairway and the outcrop was studied during field work on the east coast, lower Manzanilla. The outcrop displayed thick conglomeratic beds with chert boulders that were up to 10 cm in diameter. The top of these beds which were approximately 1 m in thickness appeared to have been influenced by near shore currents which winnowed away the finer grained sediments leaving more clast supported layers behind which were not well sorted. The cherts there also maintained quite polished surfaces which was possibly due to sand grain abrasion during drier periods, possibly associated with a displaced or irregular ITCZ, which could have created more arid conditions locally. These chert boulders are more than likely sourced from the Naparima Hill Formation from the present day Central Range, which is deep water argillite with known chert deposits formed most probably through a biological-sedimentary processes where large number of diatoms and radiolarians accumulated, dissolved and recrystallized to form chert nodules or layers. Subsequent uplift and erosion of the Naparima Hill Formation could have formed alluvial fans and associated debris and hyper concentrated flows leading to the formation of the Cunapo conglomerates.

Structure

The AO4 Anticline typifies an intensely deformed unit both structurally and stratigraphically. Structurally, the anticlinal axis has been dislocated at numerous repetitive sections along the anticline by tear faults with almost vertical reflections (Figure 16 cross-sections) which originated from as far deep as the Navet detachment surface at -1.5 km depth, continuing all the way to surface. These faults showed vertical displacements through normal and reverse faulting regimes of up to 30 metres which dislocated and compartmentalized numerous sand packages creating a series of structural traps. This reality is further complicated by bifurcations and anastomosing networks which originated from these tear faults creating a profoundly unique faulting system which can only be described as "perplexing" due to its complicated networks. This is best seen on seismic. Apart from vertical displacements, these tear faults also revealed a significant lateral displacement component. This is observed in the outcrop cross-section along OAS Quarry which showed significant deformation and faulting within a minor segment of the anticline.

These lateral displacements prominently unhinged the anticlinal axis at repetitive sections along the study area with sand package continuity being noticeably disconnected. To further complicate matters, thrust faults with north/northeast detachments as in the Navet were inferred based on the geological evolution of the region. These low angle faults strongly influenced and initiated younger faulting regimes such as the tear faults. These are best seen on the sand top structure maps for the four sands mapped the SH1, SH2, SH3 and SH4 both done manually and using PETREL as a different methods structural contouring (Figures 17, 18, 19 and 20).

The SH1 structure maps both show a prominent WSW-ENE anticline which is obviously dissected by curvilinear NNW-SSE tear faults. Faults are manually introduced into the Power Point map based on PSI values, lowest known oil, production data, contour intervals, and sand signatures on electric wireline logs. The PETREL map does not highlight faults but a quite obvious fault patterns can be inferred where the axis of the SH1 anticline is dissected to the SSE. Thrust faults at the level of Navet is implied as the AO4 thrust seen in the PowerPoint map. There appears to be a significant amount of rotation during dislocation along these tear faults as is seen on eastern part of the Figure 17b structure map.

These maps are contoured using different techniques but show some very interesting trends, as the SSE migration of the anticline from SH1 deposition time as seen in Figure 18b. Substantial accommodation space is created to the north/northwest of anticline with some developing to the south and the structure is again seen to be dissected by NNW-SSE curvilinear tear faults. These faults are manually incorporated into the PowerPoint structure map and were associated with the kinks in the anticline axis as seen in the PETREL map. This structure also appears to have developed more complexities as its predecessors.

The structure of the SH3 was most certainly more complicated than its predecessors. Faulting appears to be more extensive and this was associated with the anatomising tear faults which have now considerably fragmented the structure with its vertical and lateral components. There appears to be more structural lows or accommodation space associated with the SH3 structure. Structural lows are now prominently observed on both flanks of the main anticline as compared to the deeper structures.

Structural complications remained visible at the time of SH4 and the anticlinal axis appeared to have migrated back NW associated with another phase of tectonic deformation. The axis is again unhinged by tear faulting and from the time of SH3, the structural lows appeared to again migrate south with lesser amounts occurring to the north east. A potential component of rotation was noted to the eastern half of the anticline in the PETREL map. This rotation although minor appeared on all the anticlines. Apart from structural regimes, stratigraphic complexity is by no means absent with strong evidence of pinch-outs, fluctuating sand thicknesses and paleobathymetry all involved in this system. Surface evidence of pinch-outs is best exposed in the Golconda Interchange outcrop as seen in Figure 21.

Sand maps and provided reinforced evidence for the complex horizontal and vertical component of faulting in the area but also showed significant stratigraphic relationships. It was clearly observed that sand thickness fluctuates during deposition as seen in the SH1 sand map and SH1 net pay maps. Thus, sand deposition is greatly influenced by growing thrust faults and paleobathymetry in a tectonically active basin. SH1 sand and net pay maps clearly illustrated evidence of sand thinning to the ESE, with a bifurcation of the main channel of deposition into two less eminent offshoots. Thicker sands are guided into these channels with the bifurcating agent acting as an obstacle. These channelised processes are consistently seen throughout the other sand and increase with shallowing as seen in the net pay maps especially in the SH4 where prominent bifurcations occurred.

These sand maps displayed similar patterns but with a different contouring technique using PETREL. The thick sand deposits were quite obviously channelised and significantly influenced by faulting regimes. Structure of the seafloor appeared to be a major controlling factor, forcing the copious sand deposits into the structural lows.

Paleotopography maps were developed by calculating the true stratigraphic thicknesses between the top of two consecutive sand tops (top SH1 and top SH2) for all the electric log sand picks together with 3D and 2D seismic sand top picks (Figures 22-23 and 24-25). Further, with the assumption that thicker stratigraphic units were deposited in structural lows on the sea floor, these thickness values were multiplied by -1 to acquire a negative surface. These values were contoured to create paleobathymetry maps. From the SH2 and SH3 paleobathymetry maps (Figures 29-31), it was observed that the seafloor was by no means ubiquitous during the deposition. Poignant structural highs are seen migrating to the SE from the SH1 through SH2 to SH3 paleobathymetry maps and this is consistent with the oblique collision of the Caribbean Plate with northern South America before 10 Ma (Pindell, 2007 and 2009). This migrating anticlinal fold is associated with the creation of accommodating space on either limbs with the greater depositional space occurring to the southern flank of this migrating bathymetric high. The bathymetric lows become more even throughout the area from SH2 to SH3 and accommodating space is now confined to shallower depressions as the deepest depocentres have now been propagated south as the oblique collision of the Caribbean Plate continues. These paleo-highs are aligned WSW-ENE and are more than likely controlled by growing thrust faults with some components of lateral unhinging being formed by growing faults.

With the assumption that thick sand deposits are associated with paleobathymetry lows during deposition, the above sand maps were overlain above a featureless paleobathymetric map as seen in the SH2 net sand map (Figure 23) being overlain above the SH2 structure map. This was validated from the observed thicker sand units conformed to paleobathymetric depressions as seen in where AO 108, AO15, AO12 and AO100 are located. Thinner sands were associated with bathymetric highs as in AO31, AO102, AO19, AO 24, and AO25. The area to the south east of

AO29, showed a thin sand overlay and this is due to the fact that no well-control exist in this area and if a well were to be drilled here, a thick sand unit would be expected.

The same phenomenon was observed when the SH4 (Figure 25) sand map was overlain on the SH3 structure map with the thickest sands in during this episode of deposition being associated with wells at the centre of the map in areas as AO8, AO109, AO105, AO102, and others. As compared to SH1 paleotopography where greater accommodation space was observed in more prominent, confined and deeper bathymetric lows, this map however showed the sands are more uniformly deposited within shallower but more expansive bathymetric lows. The larger more pronounced hanging wall synclinal folds have migrated south to the Herrera fairway where larger sand packages are being deposited in larger fairways.

Discussion and Conclusions

Existing well-file biostratigraphy from 1956 and 1986 both classified the Retrench sandstones to be reminiscent of Early Miocene deposits. Persad (2011) again classified these as Early Miocene which like the Brasso, Nariva and Herrera sandstones were deposited in a series of east-northeast/west-southwest Lower Miocene foreland uplifts and foredeep basins with younger reservoirs trending to the south/southeast. Likewise, Pindell and Kennan (2007) suggested imprecisely that these are Middle Miocene deposits like the Penal Barrackpore and Balata Herrera and Karamat sandstones and shales which were imbricated by ramped up Cretaceous and Nariva thrust slices from the north in the Late Middle Miocene. These deposits of the Oropouche Oil Field are now specifically dated to be N9-N10 (*Gl. foshi peripheroranda* and *Gl. foshi foshi* planktonic foraminifera zones Trinidad) of the Early-Middle Miocene and are now more genetically related to the Herrera sandstone which is a Late Early-Middle Miocene deposit.

The Golconda Retrench sandstone outcrop (GIRSO) which is aligned to a similar outcrop as described by Kugler (1958) has been dated to be Early Miocene (20 mya) in the *Gl. Insueta* zone or the N7 of the Cipero Formation. (Farfan and Wilson, 2015). This GIRSO is therefore considered an older reservoir in comparison to the N9-N10 Oropouche wells sandstones immediately to the south along depositional strike. In line with the southward advancement of the deformation front and its associated asymmetric open east facing foredeep, we can now infer further turbidite events in the Southern Basin, with N5 Nariva sandstones within the Central Range, the N7 Retrench sandstones at GIRSO, the N9-10 Oropouche wells sandstones, the N11-N12 Penal Barrackpore Herrera sandstones, and the N12 Siparia/Barrackpore/Moruga Karamat sandstones.

These paradigms present numerous questions as, “Could the sandstone and shale sequences penetrated in the Oropouche Oil Field be reminiscent of the earliest Herrera (7d) which is almost absent in the Penal Barrackpore Basin?” Or, “Is it possible that the Golconda Interchange outcrop is the truest representation of the Early Miocene Retrench sandstones?” To answer the first question, it is very possible that this might be the case now that the Retrench has been precisely dated, as in quite a number of well file paleontology reports, thin layers of 7a and 7bc (<15 m) Herrera were observed below the Lengua (Gr1 and Gg7) but overlaying the 600 to 900 m thick Retrench section. It is also equally possible to speculate that the perplexing Gg24/32 zone underlying the Retrench (See Figure 16 cross-section) which has not been identified as distinctly as Retrench or Nariva, could then be possibly equivalent to an Early Miocene deposit similar in age to the GIRSO and potentially be a proper Retrench deposit but further biostratigraphy work is essential to solving and unravelling these knots. It could also be

probable that imbrication and interfingering of the Nariva Formation and Retrench could be responsible for the misunderstood Gg 24/32 zone. As for the second question, this is also conceivable and presents the fantastic opportunity to explore for earlier Retrench turbidite deposits further north of the Oropouche Oil Field.

Trinidad's geological evolution has been rather complex and its polyphase structural elements involving inherited and recycled phases of orogeny from Late Oligocene to Middle Miocene and its strike-slip dominated fault regimes since have made the area challenging to interpret (Pindell and Kennan, 2007) These transpressional and transtensional regimes formed by the oblique collision of the leading of the Caribbean Plate have developed imbricated, repetitive, en echelon thrust stacks with faults that bifurcate and anastomose from deep detachment surfaces as far deep as the Cretaceous, thus juxtaposing older stratigraphic sequences against younger. These complexities together with marls and sandstones which look almost identical makes understanding the depositional environment of these foredeep basins and their stratigraphic successions quite perplexing.

Biostratigraphy, although tedious, makes it possible to reconcile stratigraphic progressions. Emanating from this research, *Planulina wuellerstorfi* discussed above, indicated that the Retrench sandstones were deposited in a middle-bathyal (1500 m) or deeper paleobathymetric basin. This is against the earliest work by Strainforth (1948) which regarded the Cipero as deep water oozes being deposited in an open sea environment at depths of 400-500 m above the CCD and did not ascribe abyssal environment which is also inaccurate as abyssal depths are below 6000 m. An influx of middle neritic, Brasso Formation associated *Amphistegina* sp. and outer neritic *Uvigerina paravula* into the basin was observed. This obviously indicated a movement of shallow water facies into the middle-bathyal basin as seen between samples depths 313 m to 322.50 m (-1028 to1057 feet)and sampled depth 341.5 to 352.50 m (1120 to1152 ft) in Figure 3, Figure 4 and Figure 5. A modern analogue of this is seen in St. Kitts where Wilson, 2008, 2011 (as cited in Wilson, 2011) reported that bathyal assemblages around the island contained 56% allochthonous shallow-water specimens with bountiful reef species such as *A. carinata* and *A. gibbosa* as well as shallow water *Peneroplis bradyi,* and *P. proteus.* Wilson (2011) suggested the cause of this influx are hurricanes or tropical storms which are frequently experienced in St. Kitts. This is extremely unlikely in the Southern Basin and fluvial related activity where deltas prograded out from the shelf edge sweeping fine-grained sands and silts which entrained and encased these shallow water forams depositing them over the shelf edge as turbidites seems to be the formative reason for this influx. Wilson (2004) identified transgressive and regressive cycles form his study of the Central Range Brasso Formation which Kugler demarcated to be Early to Middle Miocene in age (N5 to N12 Zones) This transgression is more than likely associated with tectonic uplift in the Central Range caused by the imbrication Cretaceous Cuche rocks causing Late-Eocene to earliest Oligocene deposits to imbricate. Shelf edge olistostrome and spill-overs induced by tectonic activity, crustal loading or nearshore currents could have also be influential. An indication of fluvial activity being responsible was seen in Figure 5 which prominently identified a lower proportion of dissolution associated with an influx of *Amphistegina sp*. (vice-versa) into the basin reason being that these forams are better preserved in deltaic and turbidite flows which rapidly buried these bugs thereby protecting them from the agents of corrosion.

In trying to understand the dynamics of deposition further, these benthonic assemblage graphs were correlated with a litholog done from 91 m (299 feet) to 457 m (1500 ft) and a gamma ray log for AO117 as seen in Figure 37. An interesting but not surprising trend was observed as seen in Figure 37, where a lower API reading in the gamma ray between 313 m (1028 feet) to 352 m (1152 ft) associated with a sandy unit in the litholog, corresponds to an influx of *Amphistegina* sp. and a spike in the *Amphistegina* sp. to planktonic ratio at the equivalent depth. This interval showed a minor increase in grain size, superior sand grain concentration and oil impregnation in the AO117 litholog. These paradigms

are most logically associated with sea level fluctuations during the Early Middle Miocene where the uplifted and imbricated Central Range facies together with eustatic sea level fall caused sediments to be shed into the Retrench foredeep. DORSEC (2007), and Gohn et al. (2009) sea level fluctuation curves based on sequence stratigraphy off the coast of New Jersey which has been a passive margin setting since the early Mesozoic showed prominent close to base level seal level fluctuation during the Early-Middle Miocene. The nature of the evolution of the Central Range and Southern Bain with its imbricated orogenic evolution and the rim of conglomerates suggests that tectonics was the dominant forcing on base level fluctuations.

Catuneanu (2006) suggested that eustatic sea level changes in a basin are associated with the creation of equal accommodation space and tabular geometries within a basin. He goes further and states, tectonic related seal level changes however, stimulates (1) wedged-shaped geometries of sedimentary sequences, due to differential subsidence rates; (2) the accumulation of coarser-grained facies along the proximal basin rim in relation to the rejuvenation of the source areas; (3) differences in the maximum burial depths of the sedimentary succession across the basin, through diagenetic minerals, fluid inclusions, vitrinite reflection, apatite fission track, etc.; (4) changes in syndepositional topographic slope gradients through time; and (5) changes in the direction of topographic tilt (Catuneanu 2006). Some of these features are prominently observed as in the rim of Cunapo conglomerates which Barr and Saunders (as cited in Saunders, 1998) highlighted as interfingering southward and pinching out on the Central Range. Likewise, the coarse-grained Chaudière and Pointe-a-Pierre Formations the Central Range also supports this theory which Pindell and Kennan (2007) described as clean sandstone deposits sourced from a peripheral bulge uplifted by 1-2 km and eroded close to the edge of the South American Plate due to the Proto-Caribbean being subducted beneath South American. Further, these Nariva, Retrench and Herrera sandstones are also not ubiquitously buried and can be found at fluctuating depths within their respective fairways. Also, as seen in the GIRSO versus the Retrench well sandstones thin sections, important grain deformation and diagenetic difference as discussed earlier were observed. Finally, the sea floor bathymetry observed during deposition was continuously evolving and migrating to SSE during the Early-Middle Miocene which again strongly promotes the theory of tectonic uplift being the dominant forcing on basin deposition.

Further, Pindell and Kennan (2007), suggests that the Late Middle Miocene Retrench-Herrera sandstones and shales are turbidites deposited axial-parallel down foredeep basins, containing a significant amount of high grade from the Villa de Cura area in Central Venezuela as seen in Figure 38. Pindell and Kennan (2007) also suggests that Herrera sands are also sourced from the South American margin on the crest of the Caribbean forebulge with some proximal facies sourced from the Moichito conglomerate of the Serrania Oriental and Herrera cobble conglomerate as seen at Galfa Point, Trinidad. Urbani et al. (2005) describe the Villa de Cura area as high pressure low-temperature metamorphic suite. This is a complex nappe succession containing a northern section of meta-volcanosedimentary suites. The northern segments as in Santa Isabel contains a mixture of granoblastic non-foliated metamorphics and varied schists, El Carmen contains meta-lava and meta-tuffs with distinctive interlayered pyroxene meta-basalt and the El Caño and El Chino contains meta-tuffs. These comprise minerals such as lawsonite, albite, glaucophane, epidote, quartz and occasionally stilpnomelane, chlorite, clinozoisite, crossite and barroisite. The southern segments of the Villa de Cura contains with very low or no metamorphism with facies no higher that prehnite-pumpellyite. The basalt show island arc affinity with ranges from Middle to Late Cretaceous lavas and these units are interpreted to be an un-subducted island arc. Minerals as plagioclase and pyroxene phenocrysts, with recrystallized matrix to chlorite, albite, calcite and epidote are observed here (Urbani et al., 2005).

As discussed in section 4.3, the only minerals observed from the Oropouche Oil Field and GIRSO were monocrystalline quartz, cherts, minor amounts of feldspar and calcite in the two deepest thin sections at AO117: -1220 to -1239 m and AO118: -823.50 to -834.50 m. No evidence for any of the metamorphic minerals associated with the Villa de Cura nappe was observed, strongly indicating that this is not the source of the sandstones. The Oropouche Oil Field thin sections are intensely deformed quartz grains and although a couple grains exhibited a few polycrystalline tendencies, these were more associated with grain fracturing rather than metamorphism. Local imbrication of the Nariva, Retrench and Herrera as well as complex faulting regimes and history looks to have contributed significantly to the deformation of these quartz grains. The cherts are also considerably less deformed than the quartz and show no evidence of metamorphism. These newly observed paradigms indicate a more local origin of these quartz and cherts as in the Chaudière, or Point-a-Pierre Formation and Cunapo Conglomerates of the Central Range (Figure 41).

Pindell and Kennan (2007) describes the Chaudière, Lizard Springs, Pointe-a-Pierre, Navet, and Plaisance as Late-Eocene to earliest Oligocene, clean continental margin sandstone and shale sequences east of the Urica Fault with no evidence of detritus from the Caribbean Plate. Pindell and Kennan (2007) goes further to suggest that these clean sandstone deposits were sourced from a peripheral bulge which was uplifted by 1-2 km and eroded creating a subaerial unconformity close to the edge of the South-American Plate due to the Proto-Caribbean being subducted beneath the South America (Figure 40). Advancing bulges from the Proto- Caribbean were then amalgamated, became immobile and later overridden by new migrating forearcs. These quartz were therefore more than likely monocrystalline which experienced only minor amounts of metamorphosis and is seen in the Point-a-Pierre quartz arenite thin sections which are dominated by monocrystalline quartz with only a few polycrystalline quartz grains observed. This sandstone has been intensely packed showing evidence of grain fracturing, grain migration and pressure solution influenced possibly by imbrication of the underlying structures but are in no way as deformed as the Retrench. This deformation seen in the Retrench (well-samples) quartz appeared to predate deposition in the basin as the cherts profoundly less deformed which indicates a polyphase reworking of the quartz into the Nariva which as suggested by Pindell and Kennan (2007) has been imbricated into 5-6 stacks by the underlying Cretaceous. This now intensely deformed grains were then deposited into the Retrench and Herrera SE migrating fairways. This creates a logical mechanism for the significant deformation of these grain.

The cherts are not metamorphosed and based on grain paradigms discussed earlier, a more local source such as the Cunapo Formation which according to Saunders (1998) outcrops in the eastern Central Range and southern flank of the Northern Basin seems to be the most logical proximal source. Barr and Saunders (as cited in Saunders, 1998), describes the Cunapo Formation as a great sweep of coarse material within the Northern Basin and those that are penetrated are challenging to date but can be seen interfingering with other formations southward. The recent uplift of the Northern Range is also seen as being responsible for shedding conglomerates southward. These conglomeratic chert beds is more than likely sourced from deep water Naparima Hill Formation argillite which contains chert beds with opal as seen at San-Fernando Hill itself (Farfan, 2014). Nichols (2009) also suggested that black and brown cherts which are associated with high levels of organic matter. This is most certainly present in the Naparima Hill Formation and the cherts in all the thin sections were seen to be black and brown which was an excellent clue. Subsequent uplift and subaerial exposure of Cretaceous Naparima Hill in Central Range due to south driven imbrication could have later exposed outcrops like those seen at San-Fernando Hill which was then eroded and reworked into the Cunapo Formation. Therefore, it is suggested these conglomeratic beds were more prominent and exposed in the Early and Middle Miocene and sourced the cherts seen in the Nariva, Herrera and Retrench foredeep basins. A supporting piece of evidence of this is discussed above where the Cunapo Conglomeratic beds

of Lower Manzanilla are reworked by nearshore currents which could have willowed these finer grained cherts away into the middle-bathyal basins.

Deville et al. (2013) and Callec et al. (2010) suggested that classic sedimentation patterns for offshore deltas and deep-sea fans on passive margins which are defined by profound marine erosion processes at the platform border through shelf-edge canyons, bifurcating channel-levees turbidite system along the continental slope (deep-sea fans), and lobe like deposition on the abyssal plains can no longer be associated with active margin regions as the Orinoco, Indus and Ganges. Callec et al. (2013) continues and stated that extensive migration of the siliciclastic source, tectonic mobility of the region and continuous deformation drastically influences location and geometry of depocentres. This is certainly so in the evolution of the Retrench continued with deposition into a complex of evolving basin floors. The only notable work done to understand the evolution of bathymetric features within the southern basin and restore depositional surfaces was by Moonan (2011) where PETREL and Midland Valley MOVE geophysical software was used in in reverse modelling the growth of the Penal/Barrackpore Anticline by restoring deformation observed on multiple detachment surfaces from Pleistocene to Middle Miocene. The restoration process included rotation of beds along thrust faults, removing the throw of the Penal/Barrackpore Anticline overthrust and Debe/Wellington sub-thrust faults and assuming deposition on bathyal slopes of 1 -2 degrees. A vector map was generated to allow for the restoration of individual Herrera sand packages in wells between the restored seismic sections. The results of this work highlighted depositional regimes, sand thickness relationships, foreland propagation, accommodation space and bathymetric relationships. A similar concept was applied here as discussed above, but stratigraphic thicknesses were used to reconcile paleobathymetry as the study area was too limited to reconfigure shortening and significant folding. Within the Retrench fairway, it was observed that paleobathymetry significantly influenced sand deposition where thick units were deposited in paleo bathymetric lows and thin units culminated against growing bathymetric highs as seen in the SH2 sand map overlain on SH1 structure and SH4 sand map overlain on SH3 structure. Similar trends were observed by Moonan (2011) in the Penal Barrackpore field where the absence/reduced N11-N12 Gr7bc Herrera was caused by thinning against the anticlinal crest. These seismic scale observations along with outcrop examples strongly suggest a syn-kinematic depositional system. This should be a constant throughout this active margin and Callec et al (2010) also observed in the south of the Barbados accretionary prism where sea floor topography influenced syn-tectonic sedimentation of the Orinoco turbidite.

Accommodation space observed decreased from the deepest sandstones with the thickest deposits occurring as than SH1 and couple others below it. This was caused by a greater magnitude of subsidence in these units which confined turbidites to deeper undulations on the seafloor which migrated south/south-east as the oblique collision of the CP continued. As these SE advancing bathymetric highs coalesced, their migration then slowed as compared to those ahead, began to uplift due to isostasy and this caused accommodation space to become more even across the bathymetric surface as seen in the SH3 and SH4 sand maps which are more evenly distributed as compared to its predecessors. This has been where the SH4 sand was draped on the SH3 paleobathymetry map. Because the magnitude of subsidence decreased with merging anticlines, accommodation space also decreased from SH1-SH4 deposition. Moonan (2011) observed a similar trend where the accommodation space for the earlier (deeper) Herrera 7bc being greater than for the later 7a. Moonan (2011) further highlighted areas where sands were inferred to be spilling from the restricted northern syncline to the broader southern and as such would have reduced relief significantly. Callec et al. (2010) saw similar paradigms in the Barbados where the levee deposits locally pinched out toward folds and mud volcano edifices. These findings together with the SH1-SH2 and SH3 which migrated to the SE, correspond to the oblique collision suggested by Pindell and Kennan (2007 and 2009) and goes further to show paradigms occurring during deposition endures from the Retrench into the Herrera fairway with the

migration of these basins. These trends are also seen in the SH1 through SH4 structure maps where a major anticline at SH1 time migrated SE and was subsequently replaced by an advancing syncline at SH2 and SH3 period which was later replaced by a smaller more complex anticline at SH4.

The sand maps further support the decrease in accommodation space from the deeper units as seen in the SH1 sand and net pay maps where thicker sands were deposited in a more confined but deeper channel. The SH2, SH3 and SH3 sand and net pay maps showed sands which are less confined to channels. Catuneanu (2006) suggested that turbidites are similar to rivers with coarser more channelised sands with channel fills occurring as coarser, sandier deposits favourably trapped within the channel during the flow, relative to levee deposits, and can potentially form good and continuous reservoirs. He goes on to suggest that these systems are complex and show sinuosity like meandering channels where levees are often breeched to form sand waves or frontal splays or sediment waves which are related to secondary flows that breech the main depositional system during deposition and are usually associated with finer-grained sediment fractions relative to their levee deposits. Therefore, away from the main channel, reservoir quality diminishes and are associated with the famous term “ratty sands.” In this basin however, this channel pattern seems to be secondary to or superimposed on paradigms discussed earlier but have been observed to increase their presence in the SH2 and SH3 sand and net pay maps, with bifurcating channel in the SH4 caused by obstacle on the sea floor. The thickest SH1 net sand and pays are deposited to the centre of this channel, whereas the rest revealed the thickest sands occurring to the southeast of the channels thinning to the northwest which is in another indication that the greeter accommodation is migrating south and obstacles are increasing with younger deposits. Thin sands are therefore best associated with bathymetric highs and lesser with secondary flows. Further, sand packages above the SH3 more frequent with smaller intervals between and this could be due to a more tectonically unstable basin which influences more frequent spill overs, olistostrome and infills from outside or within the fairway. Callec et al. (2010) saw that channel sinuosity is highly dynamic as seen in south Barbados due to the tectonic deformation of the accretionary prism morphology of the sea floor but the Retrench basin is much more confined and hence sinuosity is a significantly more restricted.

Now that strong stratigraphic relationships have been developed, it is imperative to understand the structural regimes observed and how they have evolved and their impact on compartmentalization of reservoirs. From the manual structure maps done using electric wireline logs as described earlier, the major faults mapped appear to be tear faults that dislocated the anticline axis at numerous points. These discordant faults cut through SH1 straight to SH4 and propagate all the way to the surface, with their origin as deep as the Navet detachment surface. These are also described for the PETREL structure maps which show very similar configurations with indications of more complex faulting. These are complex faults with lateral and vertical components which involve both normal and reverse faulting with overthrusting and smaller dislocations superimposed on formations as seen in the electrical wireline cross-sections and the M2 Ring Road outcrop. These are complex faults which bifurcate and anastomose intensely and are a product of the Caribbean Plate interaction where transpressional related thrust and reverse faulting, and subsequent transtensional stress associated normal faulting after 10 mya with further inversion have contoured reservoirs into apparent labyrinths. From the structure maps it was inferred that every 300 metres, major NW-SE trending curvilinear faults occurred. These major faults seem to be the source of smaller superimposed fault networks which have created essential triangle traps but have also complicated exploration. Exploration must therefore incorporate wireline logs and seismic in ensuring that patterns outlined here are captured and exploited.

Through this sand structural and stratigraphic analysis, six drilling targets were suggested, as seen in Figure 22b for the SH1 sand as this has proven to be the most prolific producer in this area and has been largely underexploited. Potential drilling locations orthogonal and east of

AO91, AO8 and AO19, to the NE of AO99 and two more risky but intriguing targets to the SSE of AO108 and south of AO24 were chosen. Early drilling campaigns sought out the SH1 but were at a disadvantage with no seismic data, significantly less well logs and files and an incomplete understanding of the area's geological evolution. From this assessment it has been observed that these sands are channelised deposits forced into paleobathymetric lows, so a drilling campaign must first focus on finding the thickest sand trends which have shown to produce exceptionally well as in the AO8 well which produced in excess of 500,000 barrels of oil from the SH1 sand, the AO17 which produced in excess of 221,102 bbls, and AO19 which produced 103,663 bbls.

The real challenge, though, is ensuring that the proper drilling locations are chosen which are not too down-dip as in A0109 which only produced 5,176 bbls or AO99 which was even further down-dip and produced zilch. Drilling on exactly the crest of the anticline should also be avoided as these can be subject to intense anastomosing faults which could unhinge the thick sands. It is essential to remember that these structures have had a long history of deformation which makes them difficult to predict with complete certainty as seen in A091 which penetrated the thickest sand but only produced 2,822 bbls or A018 which still produced 47,662 bbls even though it penetrated a thinner sand than AO102 which produced 8,536 bbls. The thinner, shallower SH2, SH3 and SH4 sands are much harder to predict as they were deposited in smaller, less confined accommodating spaces and even though A012 produced 369,183 bbl from the SH4 sand, it is still too risky to go after these targets alone, especially as faulting increases in complexity with decreasing depths. The SH1 targets between 600 to 722 m, and potential deeper sands as in the AO44 sand must be top priority, with the appropriate reservoir evaluation. Likewise, as the shallower sands were less confined during deposition, the chance remains of encountering smaller producing sand packages, which could be oil charged, when drilling for the SH1. Multiple targets for the SH1-SH4 are almost unrealistic and not advised due to the dynamic history of deposition and deformation.

Acknowledgements

I would like to sincerely thank the folks at API Petroleum Co. Ltd., Mr. Victor Young-On, Mr. Shiraz Murf Rajab, and Miss Keone Applewhite for all their support, mentorship and guidance throughout, as well as Mr. Fawwaaz Hosein, the director at API, for making this project possible. Without Fawwaaz's vision and genuine interest in science, this project would not have been possible. Also, I am particularly grateful to Professor Brent Wilson and Ms. Ashleigh Costello for their patient mentorship with the paleontology aspect of this research, especially Ashleigh who generously loaned her microscope to me, and carefully imparted the art of picking and identifying foraminifers. Heartfelt thanks also to Mr. Richard Coutou, Hasley Vincent Ph.D., and Mr. Philip Farfan for their expert opinions and guidance during field work and their perspectives on the geological evolution of Trinidad and Tobago. Ryan Ramsook Ph.D. and Karuna Moonan also enthusiastically supported my work throughout and for their continuous mentorship, I am indeed thankful. Special recognitions also to all the folks at the Department of Geography and Geology at UWI, Mona Campus, for their mentorship, especially Rupert Green "the expert thin section architect" for his guidance and Professor Simon Mitchell "a legend of Jamaican and Caribbean geology" for his supervision. Professor Mitchell's stern, meticulous mentorship and critique of my submissions made me feel copiously invalid at times but no doubt propelled considerably my scientific writing skills and appreciation for geology, for which I am immensely grateful. Last but by no means least, I am perpetually thankful for Mr. Xavier Moonan, an enduring mentor, an exemplary geologist and a true friend. Xavier made this project possible through his negotiations with the folks at APCL, lecturers and numerous others and devotedly took time off to discuss ideas, read submissions and train me in the use of new software. His unwavering support, words of encouragement and lengthy conversations vastly fueled my passion and appreciation for geology and for all that he has done, I am eternally grateful.

References Cited

Baker, R.D., P. Hallock, E.F. Moses, D.E. Williams, and A. Ramirez, 2009, Larger foraminifers of the Florida reef tract, USA: distribution patterns on reef rubble habitats: Journal of Foraminiferal Research, v. 39, p. 267-277.

Bolli, H.M., 1957, Planktonic foraminifera from the Oligocene-Miocene Cipero and Lengua Formations of Trinidad, B.W.I. Bull. U.S. Natl. Mu., v. 215, p. 97-123.

Bolli, H., and J.B. Saunders, 1985, Oligocene to Holocene low latitude planktic foraminifera, *in* H.M. Bolli, J.B. Saunders and K. Perch-Nielsen, eds., Plankton Stratigraphy, Cambridge: Cam. Univ. Press, p. 155-262.

Bolli, H.M., J-P. Beckmann, and J.B. Saunders, 1994, Benthic Foraminiferal Biostratigraphy of the south Caribbean region: Cambridge University Press, UK.

Bowmann, S., Stieglitz, and S. Jagdeo, 2002, A Review of the Tectonics Deep Water Offshore, Trinidad/Tobago; Implications for Hydrocarbon Deposits: Spectrum Geo Inc. Technical Paper.

Callec, Y., E. Deville, G. Desaubliaux, R. Griboulard, P. Huyghe, A. Mascle, G. Mascle, C. Noble, C. Pardon de Carillio, and J. Schmitz, 2010, The Orinoco turbidite system: Tectonic controls on sea-floor morphology and sedimentation: AAPG Bulletin. v. 94, p. 869-884.

Cushman, J.A., and R.M. Stainforth, 1945, The Foraminifera of the Cipero Marl Formation of Trinidad, British West Indies: Cushman Laboratory for Foraminiferal Research, Sp. Pub. 14.

Catuneanu, O., 2006, Principles of Sequence Stratigraphy: AE Amsterdam, the Netherlands, Elsevier B.V. p. 73-104.

Denne, R.A., and B.K. Gupta, 1988, Benthic Foraminiferal Zonation on the Northwestern Gulf of Mexico Slope: A Close Look: Gulf Coast Association of Geological Societies, v. 38, p. 578-578.

Deville, E., A. Mascle, Y. Callec, P. Huyghe, S. Lallemant, O. Lerat, X. Mathieu, C. Padron de Carillo, M. Patriat, T. Pichot, B. Loubrieux, and D. Granjeon, 2015, Tectonics and sedimentation interactions in the east Caribbean subduction zone: An overview from the Orinoco delta and the Barbados accretionary prism: Marine and Petroleum Geology, v. 64, p.76-103.

DOSEC: Drilling Observations and Sampling of the Earth's Crust, 2007, The Rise and fall of sea level over the past 100 million years: The Sea Level issue, v. 5/2.

Drooger, C.W., and J.P. Kaasschieter, 1958, Foraminifera of the Orinoco-Trinidad-Paria Shelf: Report of the Orinoco Shelf Expedition, Verhandlungen Koninklijk Nederland Akademie Wetenschappelijke, v. 4, p. 1-108.

Farfan, P., 2014, Early Tertiary Petroleum Systems: Geological Society of Trinidad and Tobago. Website accessed October 16, 2016. https://www.youtube.com/watch?v=W3BriTvoMAQ

Farfan, P., and B. Wilson, 2015, 20th Caribbean Geological Conference, Trinidad, Field Guide, Central Range Carbonates, Port-of-Spain, Trinidad and Tobago. p. 4-6.

Gohn, G.S., C. Koeberl, K.G. Miller, and W.U. Reimold, 2009, The International Continental Scientific Drilling Program and the United States Geological Society: Deep Drilling Project in Chesapeake Bay Impact Structures: Results from the Eyreville Core Holes: USGS Special Paper 458, p. 805-88.

Hallock, P., 1981, Light dependence in Amphistegina: Journal of Foraminiferal Research v. 11, p. 4248.

Hallock, P., 2000b, Larger Foraminifers as Indicators of Coral-Reef Vitality, *in* R. Martin, ed., Environmental Micropaleontology, Plenum Press Topics in Geobiology, p. 121-150.

Hayek, L-A.C., and B. Wilson, 2013, Quantifying assemblage turnover and species contributions at ecologic boundaries, PloS ONE, v. 8/10, p. e74999.

Kender, S., M.A. Kamisski, and R. Jones, 2009, Early to Middle Miocene foraminifera from the deep-sea Congo Fan, offshore Angola: Journal of Micropaleontology, p. 481-517.

Kugler, H.G., 2001, Treatise on the Geology of Trinidad, Part 4, Paleocene to Holocene Formations: Museum of Natural History Basel, 309 p.

Lutze, G.F., and H. Thiel, 1989, Epibenthic foraminifera from elevated microhabitats; Cibicidoides wuellerstorfi and Planulina ariminensis: Journal of Foraminiferal Research, v. 19, p. 153-158.

Miller, K.G., M.A. Kominz, J.V. Browning, J.D. Wright, G.S. Mountain, M.E. Katz, P.J. Sugarman, B.S. Cramer, N. ChristieBlick, and S.F. Pekar, 2005, The Phanerozoic record of global sea-level change: Science, v. 310, p. 1293-1298.

Miller, K.G., and G.S. Mountain, 1996, The Leg 150 Shipboard Party, and Members of the New Jersey Coastal Plain Drilling Project, Drilling and dating New Jersey Oligocene-Miocene sequences: Ice volume, global sea level, and Exxon records, Science, v. 271, p. 1092-1094.

Moonan X.R., 2011, 4D Understanding of the Evolution of the Penal/Barrackpore Anticline, Southern-Sub-Basin, Trinidad, W.I. School of Earth and Environment, University of Leeds. p. 1-5.

Nguyen, T.M.P., and R.P. Speijer, 2014, A new procedure to assess dissolution based on experiments on Pliocene-Quaternary foraminifera (ODP Leg 160, Eratosthenes Seamount, and eastern Mediterranean): Marine Micropaleontology, v. 106, p. 22-39.

Nichols, G., 2009, Sedimentology and Sequence Stratigraphy, Oxford, England, Blackwell Publishing, p. 5-27.

Nigrini, C., 1991, Composition and biostratigraphy of radiolarian assemblages from an area of upwelling (northwestern Arabian Sea, Leg 117), *in* W.J. Prell, and N. Niitsuma, eds., Proceedings of the Ocean Drilling Program, Scientific Results, v. 117, p. 89-126.

Pearson, P.N., and B.S. Wade, 2009, Taxonomy and stable isotope paleoecology of well-preserevd planktonic foraminifera from the Upperost Oligocene of Trinidad: Journal of Foraminiferal Research, v. 39/3, p. 191-217.

Persad, K., 2011, The Petroleum Geology and Prospects of Trinidad and Tobago, Southern Energy Research Centre, The Gelogical Society of Trinidad and Tobagoo, p.1-2.

Stainforth, R.M., 1948, Description, correlation, and paleoecology of Tertiary Cipero Marl Formation, Trinidad, B.W.I.: AAPG Bulletin, v. 32/7, p. 1292-1330.

Pindell, J., and L. Kennan, 2007b, Cenozoic kinematics and dynamics of oblique collision between two convergent plate margins: the Caribbean-South America collision in eastern Venezuela, Trinidad, and Barbados, *in* L. Kennan, J.L. Pindell, and N.C. Rosen, eds., Transactions of the 27th GCSSEPM Annual Bob F. Perkins Research Conference: The Paleogene of the Gulf of Mexico and Caribbean Basins: Processes, Events and Petroleum Systems, p. 37-76.

Pindell J.L., and L. Kenna, 2009, Tectonic Evolution of the Gulf-of-Mexico, Caribbean and northern South America in the mantle reference frame: an update: Geol Soc London Spec Pub 328, p. 1-55.

Saunders, J.B., C. Roberts, W.M. Ali, and B. Eggertson, 1997, Geological Map, Trinidad and Tobago, Ministry of Energy and Energy Industries, Trinidad and Tobago.

Smith, C.A., V.B. Sisson, H.G. Ave Lallemant, and P. Copeland, 1999, Two contrasting pressure-temperaturetime paths in the Villa de Cura blueshist belt, Venezuela: Possible evidence for Late Cretaceous initiation of subduction in the Caribbean: GSA Bulletin, v. 111/6, p. 831-848.

Steele, J., 2014, The art of making thin sections: The Hammer, Quarterly Magazine of the Geological Society of Trinidad and Tobago, March, p. 9-11.

Urbani, L., L. Camposano, F. Audemard, H.G. Ave Lallemant, 2005, Southeast Caribbean Continental Dynamics Project: BOLÍVAR: Broadband Ocean-Land Investigation of Venezuela and the Antilles arc Region, Field Trip, p. 1-22.

Wilson, B., 2003, Foraminifera and paleodepths in a section of the Early to Middle Miocene Brasso Formation, Central Trinidad: Caribbean Journal of Science, v. 39/2, p. 209-214.

Wilson, B., 2004, Benthonic foraminiferal paleoecology across a transgressive-regressive cycle in the Brasso Formation (Early-Middle Miocene) of Central Trinidad: Journal of Caribbean Science, v. 40/1, p. 126-138.

Wilson, B., 2005, Planktonic foraminiferal biostratigraphy and paleo-ecology of the Brasso Formation (Middle Miocene) St. Fabien's Quarry, Trinidad, West Indies: Journal of Caribbean Science, v. 41/4, p. 797-803.

Wilson, B., 2007, Benthonic Foraminiferal Paleoecology of the Brasso Formation (Globorotalia fohsi lobata and Globorotalia fohsi robusta [N11-N12] Zone), Trinidad, West Indies: A transect through an oxugen minimum zone: Journal of South American Earth Sciences, v. 23, p. 91-98.

Wilson, B., 2008, Benthonic foraminifera indicated an oxygen minimum zone and an allocthonous, inner neritic assemblage in the Brasso Formation (Middle Miocene) at St. Fabien Quarry, Trinidad, West Indies: Journal of Caribbean Science, v. 44/2, p. 228-235.

Wilson, B., 2008a, Late Quaternary benthonic foraminifera in a bathyal core from the Leeward Islands, Lesser Antilles, northeastern Caribbean Sea: Journal of Micropaleontology, v. 27, 177-188.

Wilson, B., 2008b, Using SHEBI (SHE Analysis for Biozone Identification): To proceed from the top down or bottom up? A discussion using two Miocene foraminiferal succession from Trinidad, West Indies: Palaios, v. 23, p. 636-644.

Wilson, B., 2010, A lagoonal interlude with occasional hypersalinity in the deposition of the Early-Middle Miocene Brasso Formation, Trinidad: Journal of South American Earth Sciences, v. 29, p. 254-261.

Wilson, B., K. Orchard, and J. Phillip, 2011, SHE Analysis for biozone identification among foraminiferal sediment assemblages on reefs and in associated sediment around St. Kitts, Eastern Caribbean Sea, and its environmental significance: Journal of Marine Micropaleontology, v. 77, p. 43-44.

Wilson, B., and L.C. Hayek, 2015, Distinguishing relative specialist and generalist species in the fossil record: Marine Micropaleontology, v. 119, p. 7-16.

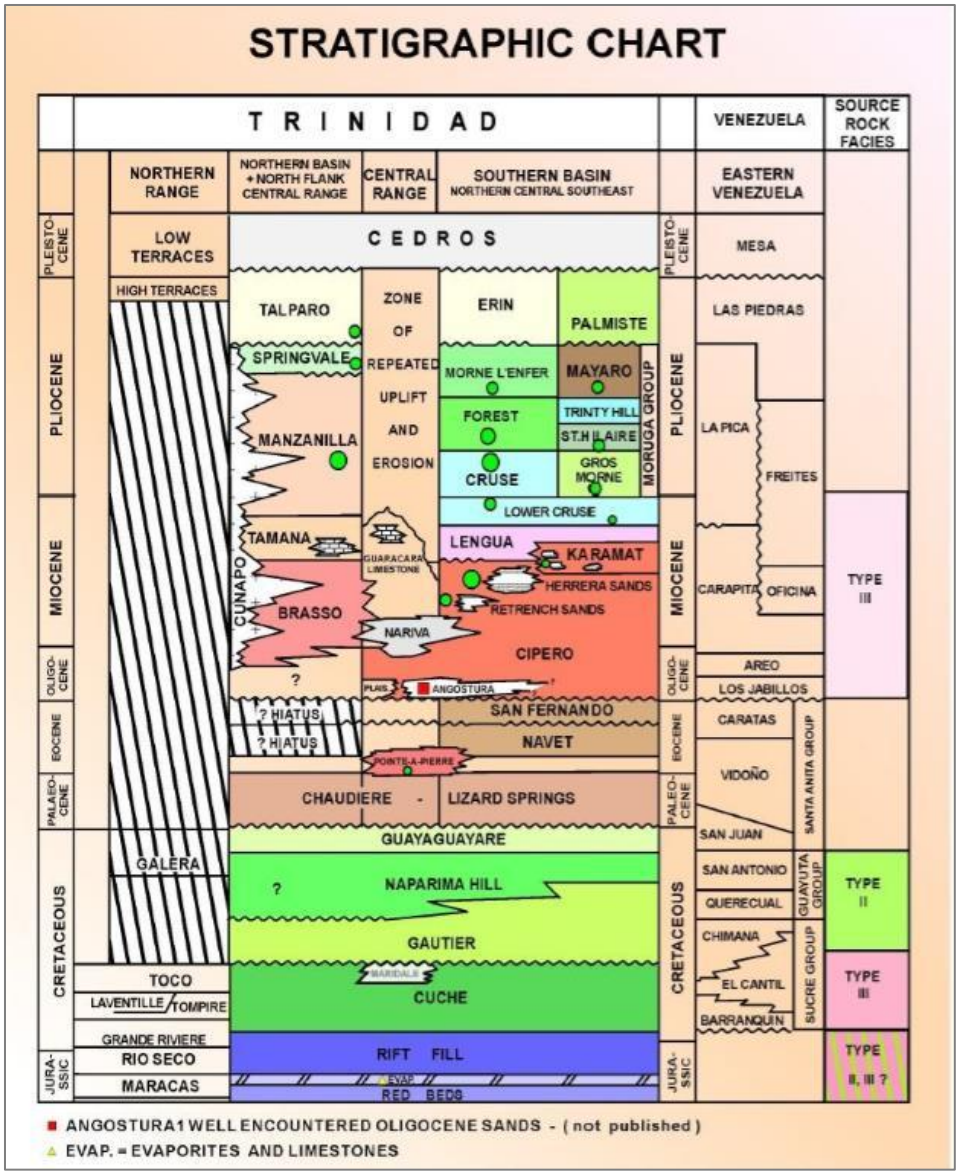

Figure 1a. Stratigraphic section of Trinidad. Modified from the Geological Society of Trinidad and Tobago (as cited in Bowmann et al., 2002).

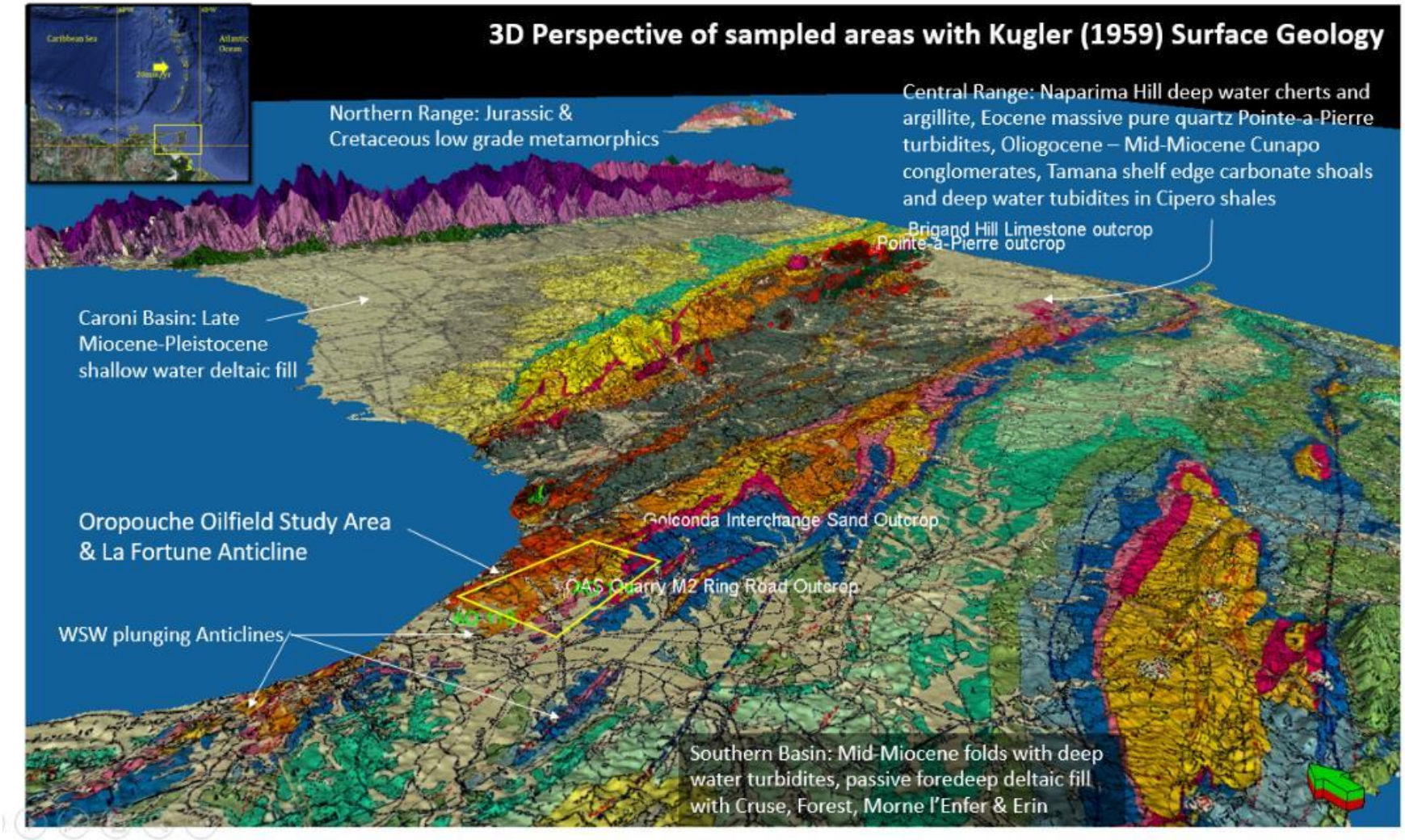

Figure 1b. 3D map of the study area region.

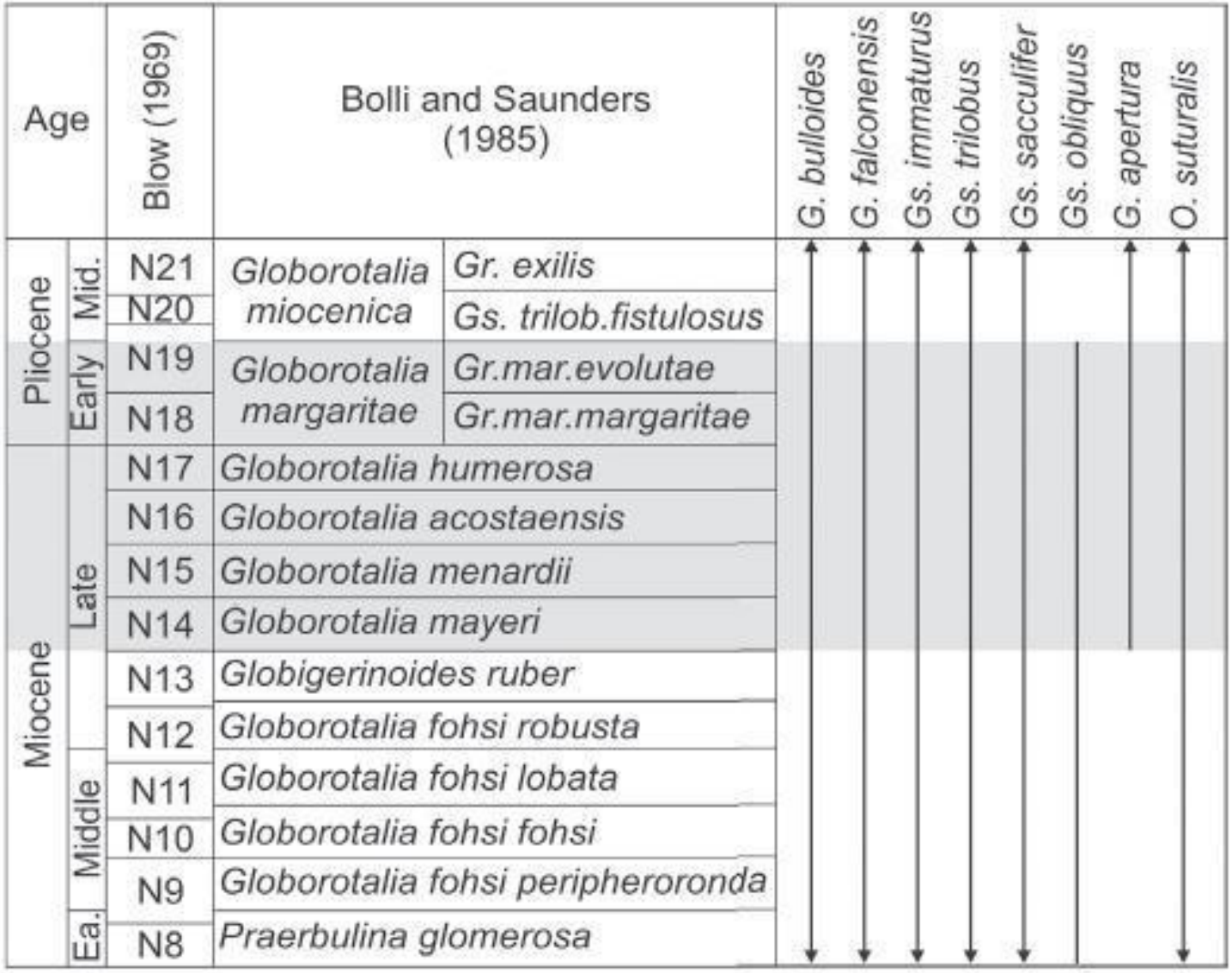

Figure 2. Neogene N classification scheme (Bolli and Saunders, 1985).

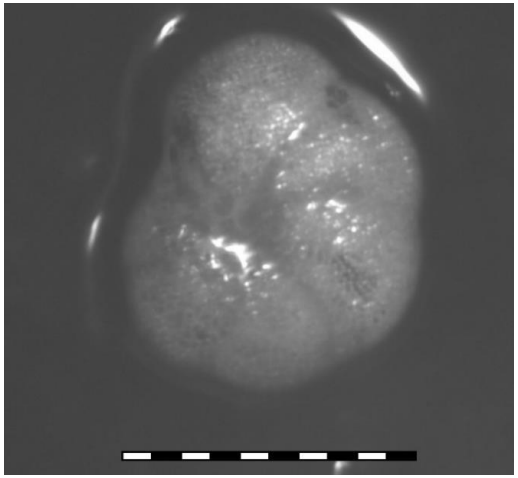

Figure 2a. Stacked image showing *Globorotalia foshi peripheroacuta.*

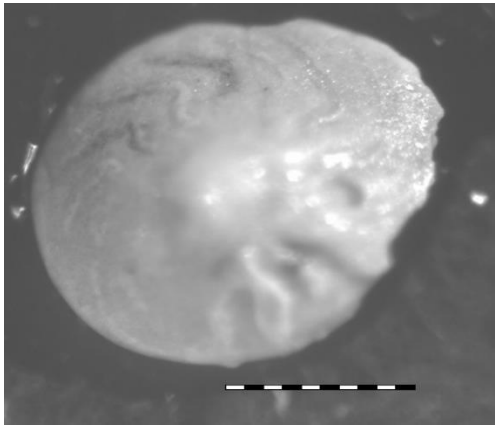

Figure 2b. *Amphistegina* sp.

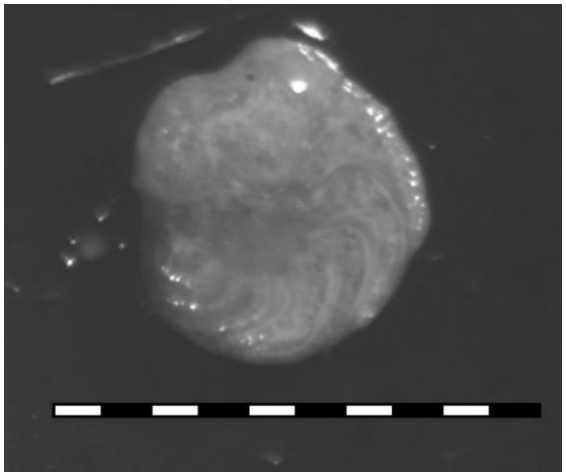

Figure 2c. *Planulina wuellerstorfi.*

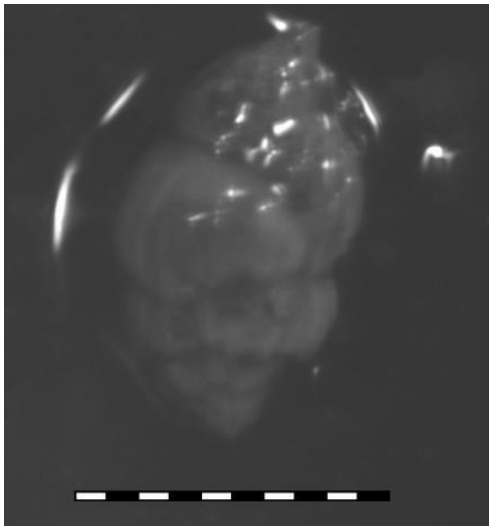

Figure 2d. *Uvigerina paravula.*

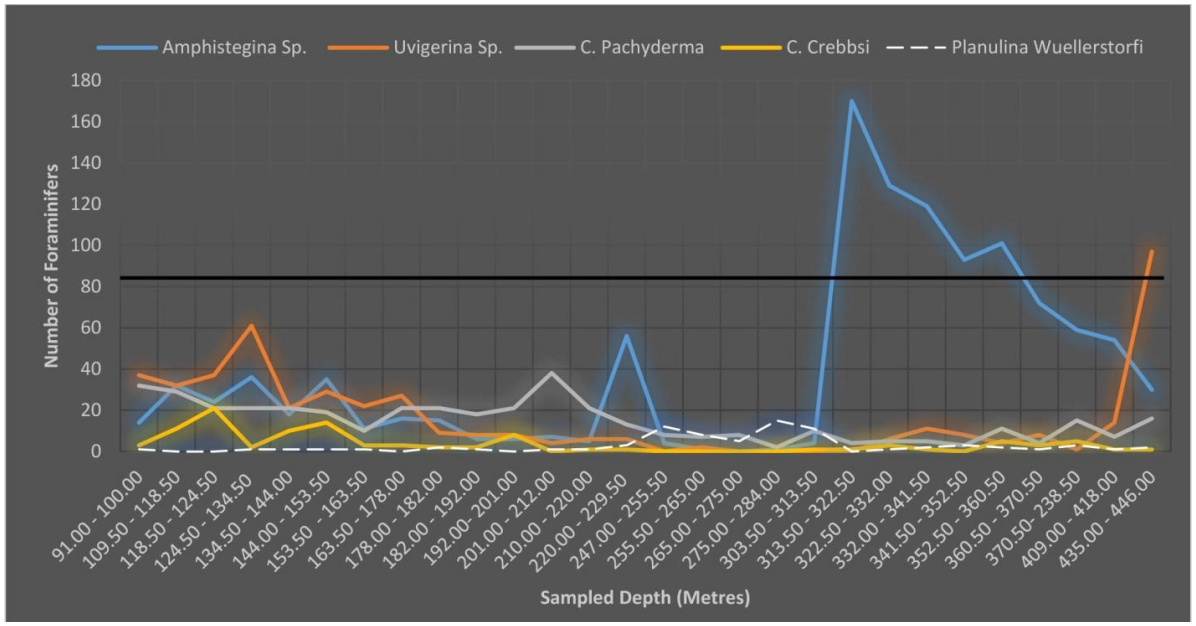

Figure 3. Graph showing five benthonic foraminiferal populations sampled.

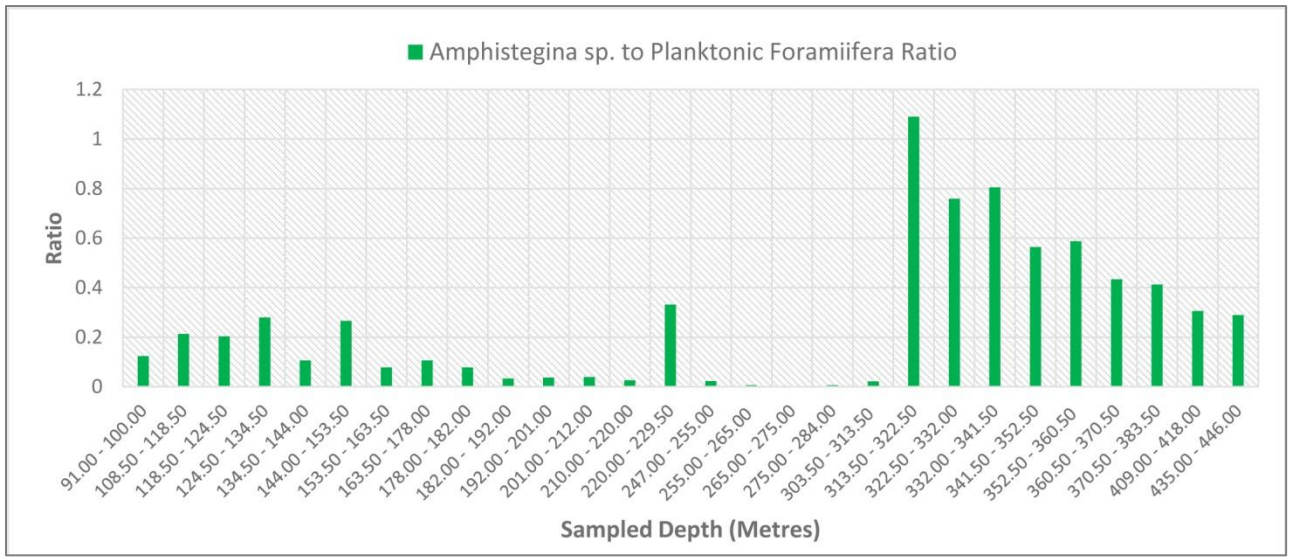

Figure 4. *Amphistegina sp.* to Planktonic Foraminifera ratio.

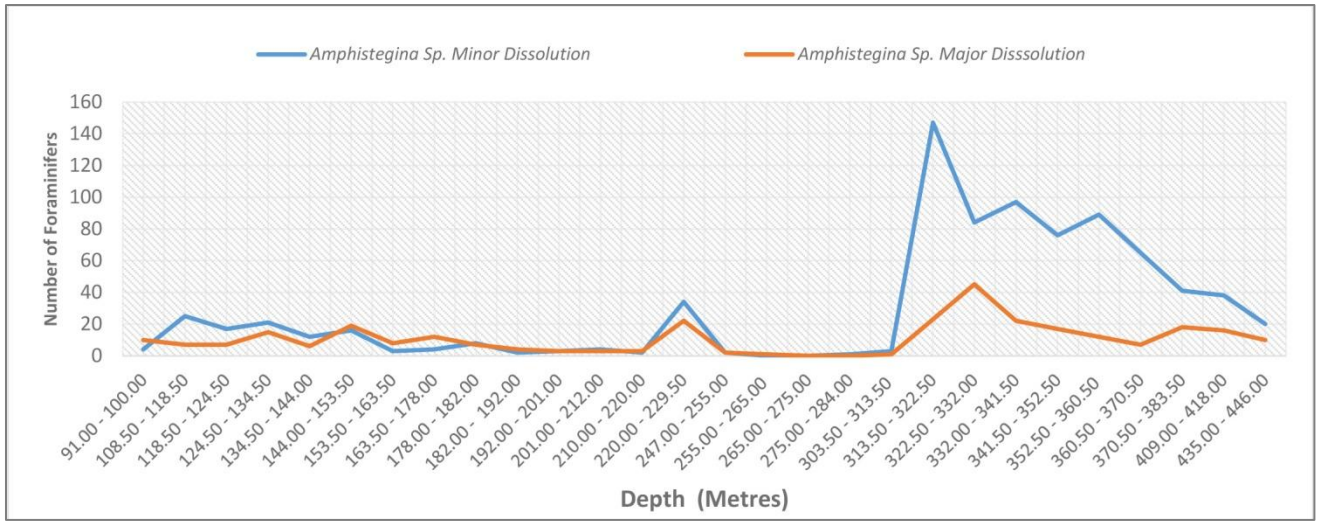

Figure 5. Major vs. minor dissolution in *Amphistegina sp.* population.

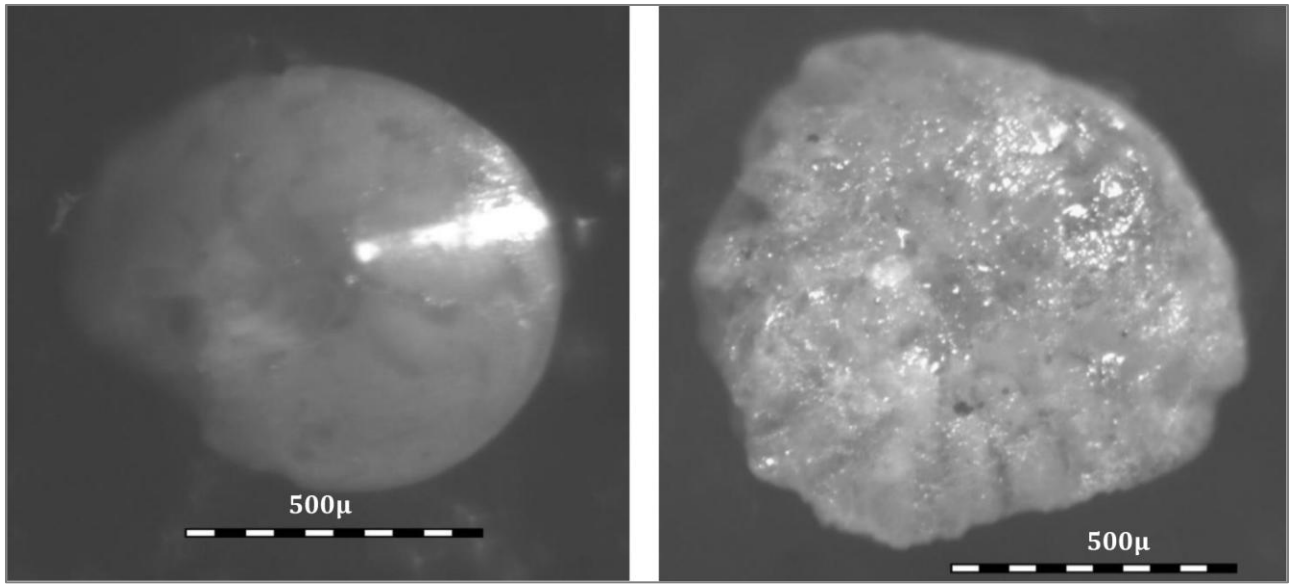

Figure 5a. *Amphistegina* sp. major dissolution (right) versus minor dissolution (left).

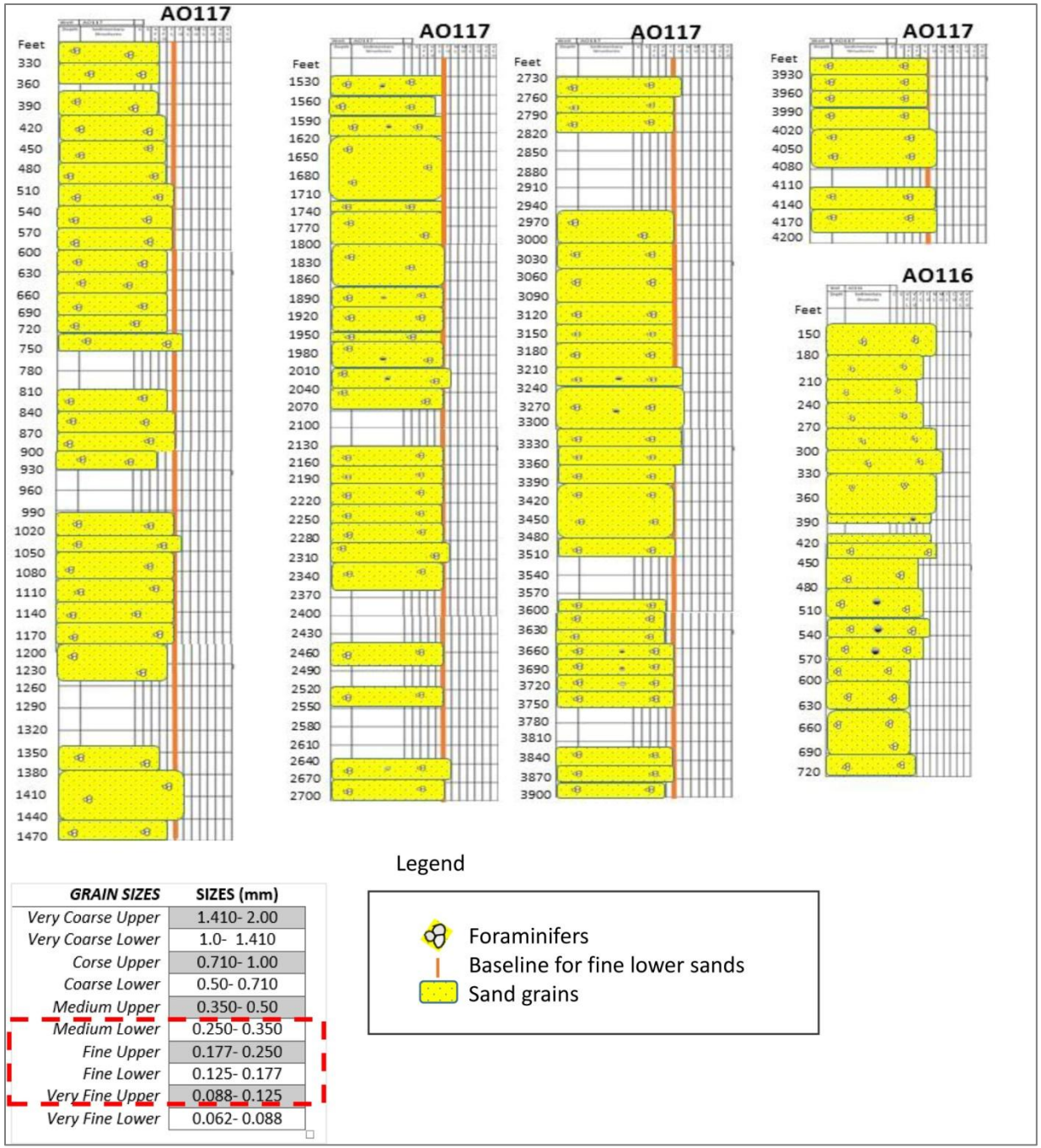

Figure 6. AO116 and AO117 lithology and grain size classification.

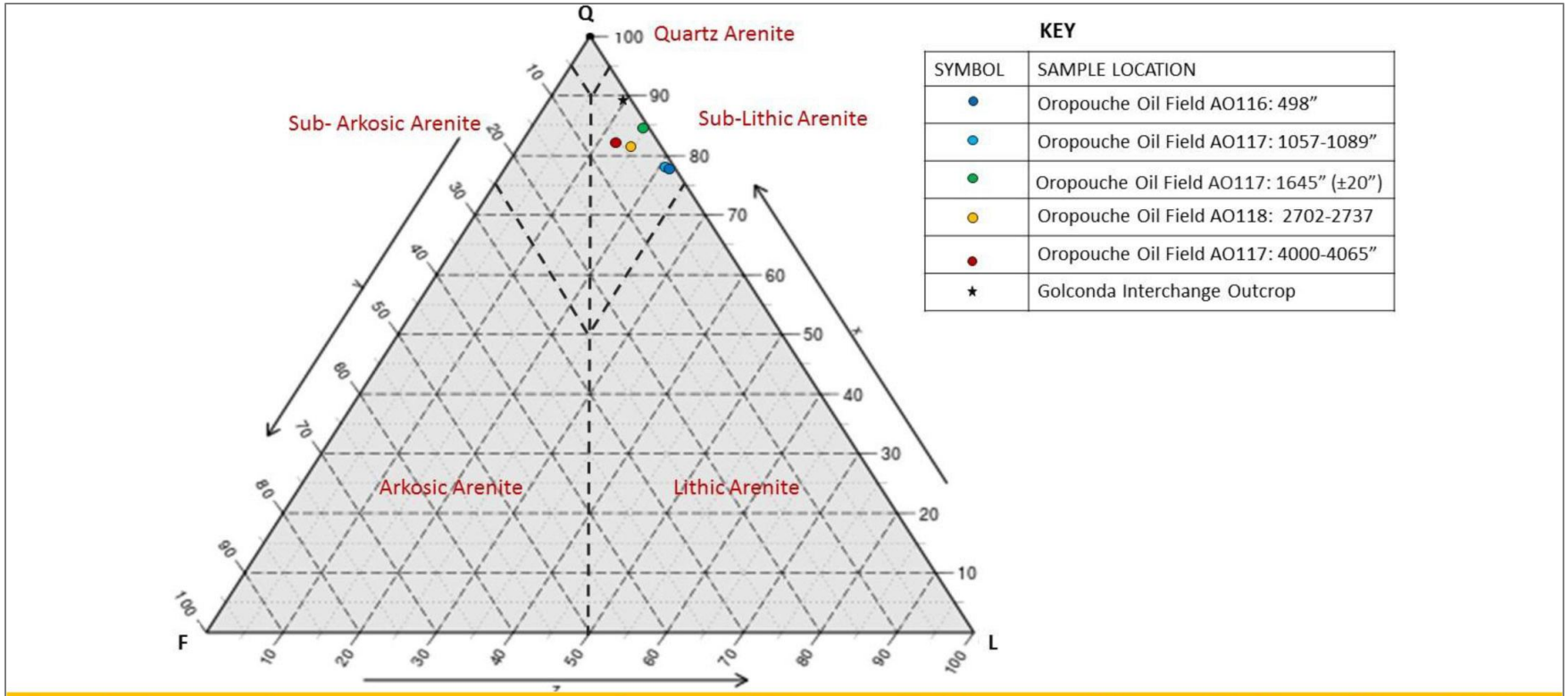

Depth (metres)	Quartz (%)	Feldspars (%)	Lithics (Chert) (%)
AO116: -145 to -156 m	78.1	1.30	20.6
AO117: -322 to -332 m	78.3	1.60	20.10
AO117: -500 m (±5 m)	84.1	0.30	15.6
AO118: -823.50 to -834.50 m	81.20	4.30	14.50
AO117: -1,220 to -1,239 m	81.90	5.5	12.60
Golconda Interchange	89.70	1.30	9.0

Figure 7. Pettijohn’s sandstone classification scheme.

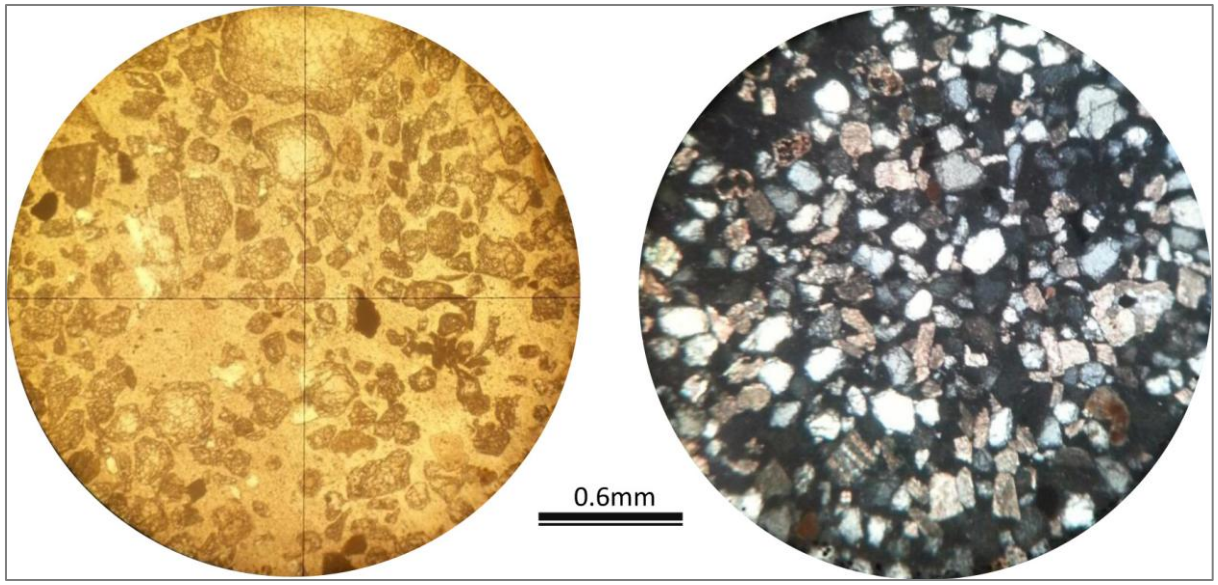

Figure 8. Retrench Sandstone AO117: -1220 to -1239 m (-4000 ft to -4065 ft).

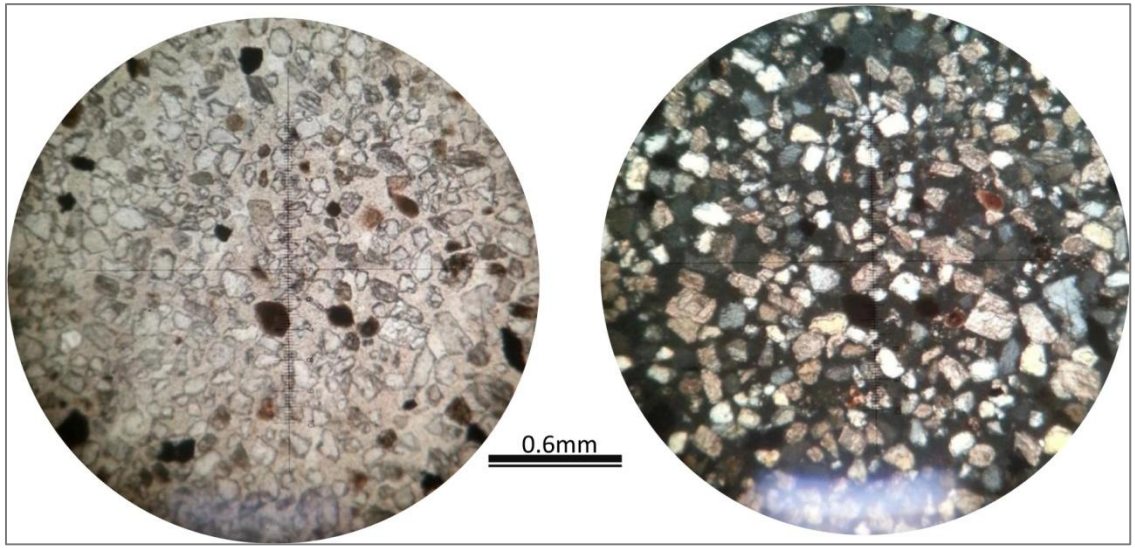

Figure 9. Retrench Sandstone AO118: -823.50 to -834.50 m (-2700 ft to 2742 ft).

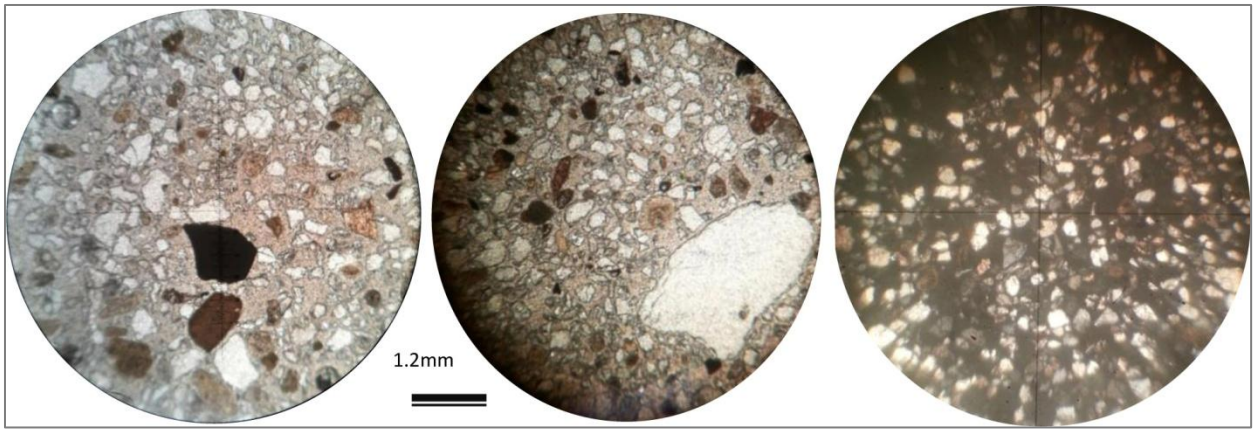

Figure 10. Retrench Sandstone AO117: -500 m (±5 m) (-1640 ft ±16 ft).

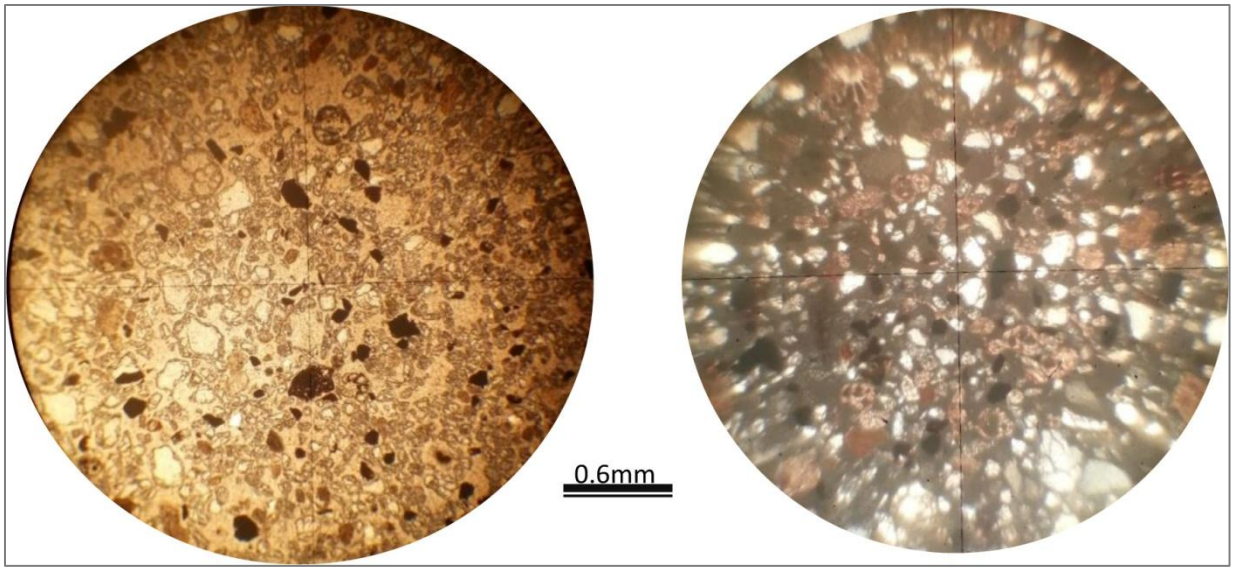

Figure 11. Retrench Sandstone AO117: -322 to -332 m (-1056 ft to -1089 ft).

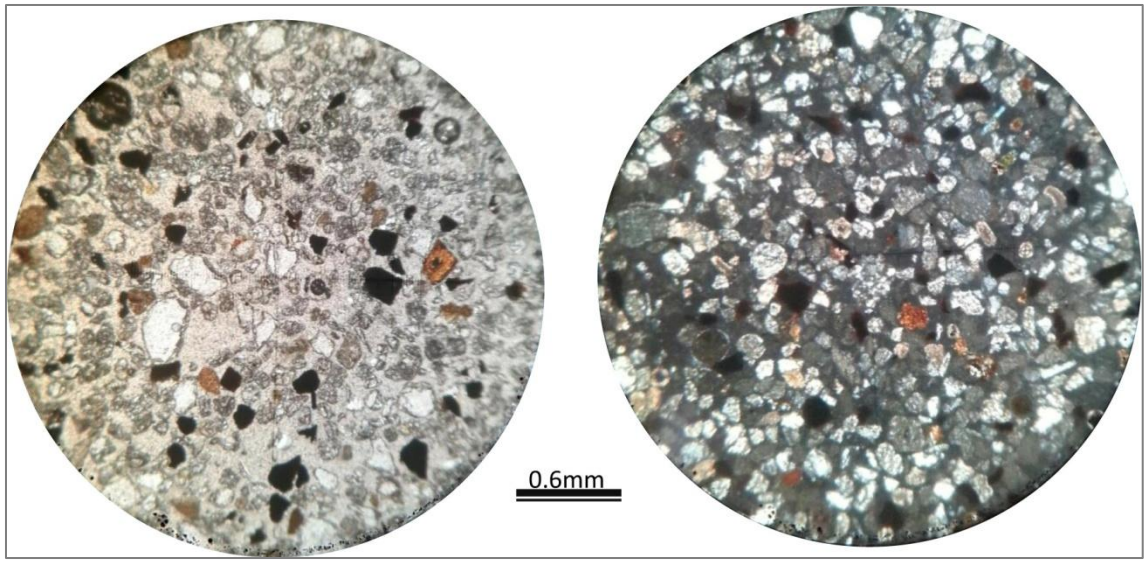

Figure 12. Retrench Sandstone AO116: -145 to -156 m (-475 ft to -511 ft).

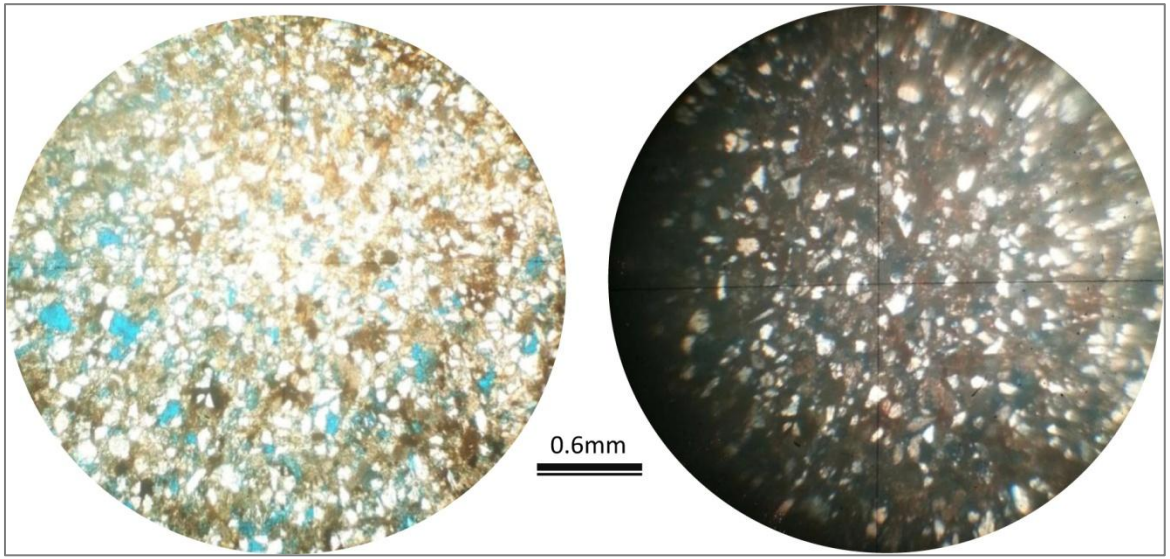

Figure 13. Golconda Interchange Retrench sandstone outcrop (GIRSO).

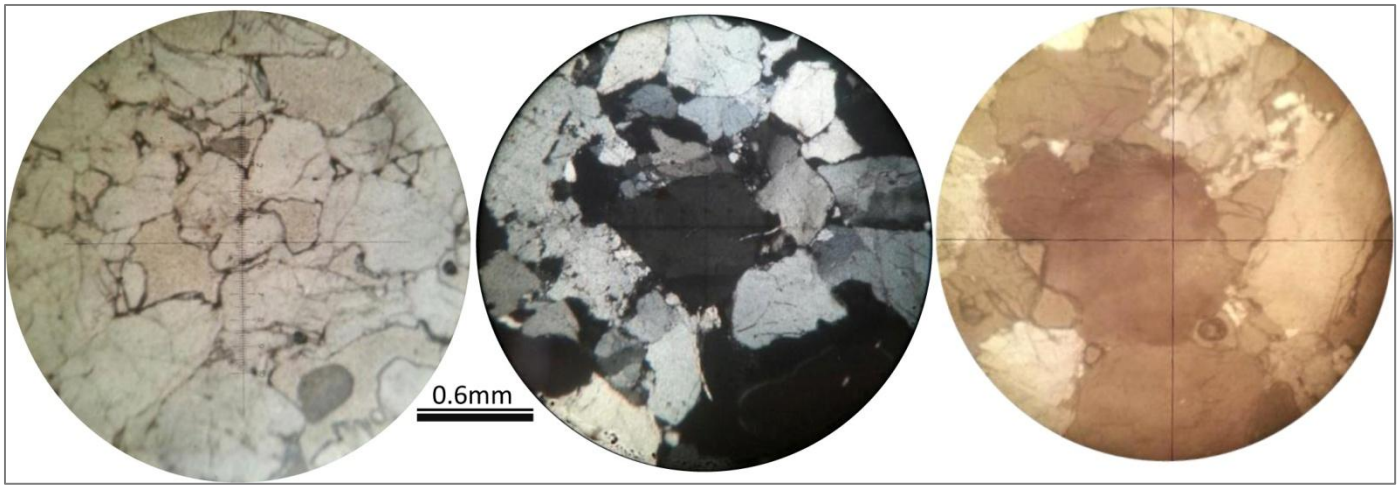

Figure 14. Sample 1 Point-a-Pierre Formation sandstone.

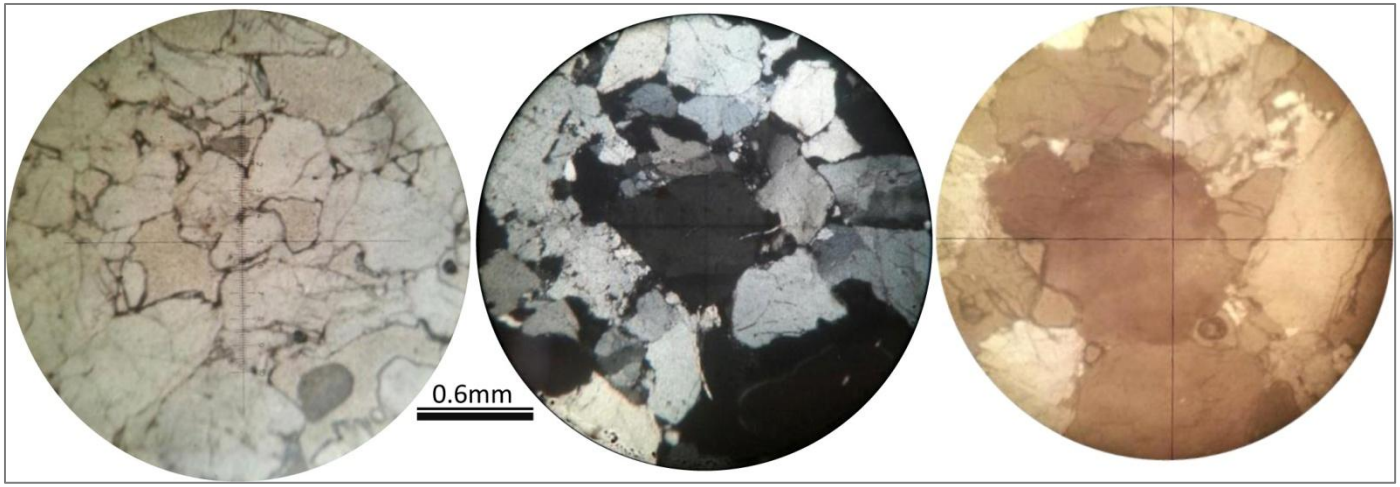

Figure 14a. Sample 2 Point-a-Pierre Formation sandstone.

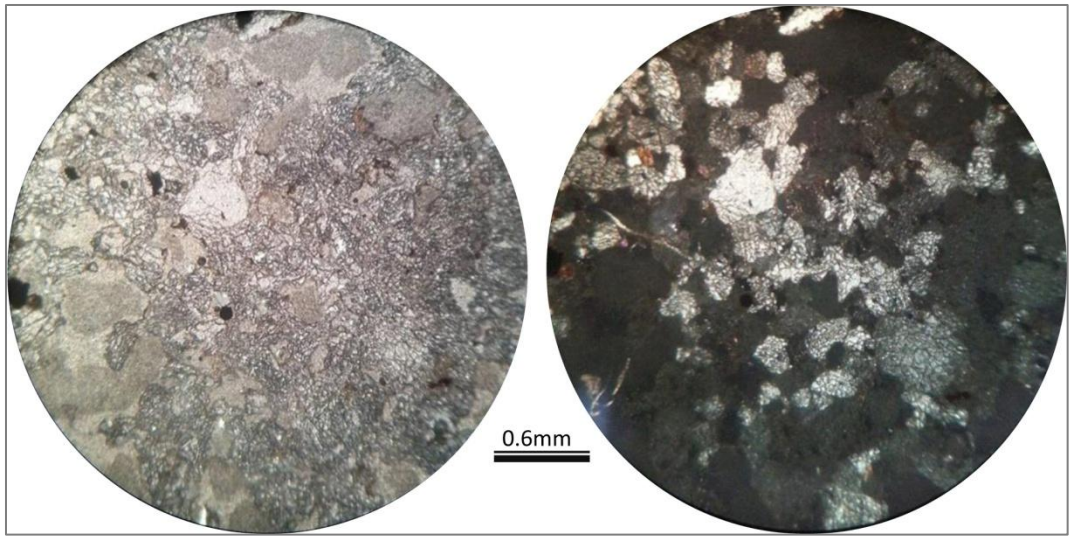

Figure 14b. Sample 3 Point-a-Pierre Formation sandstone.

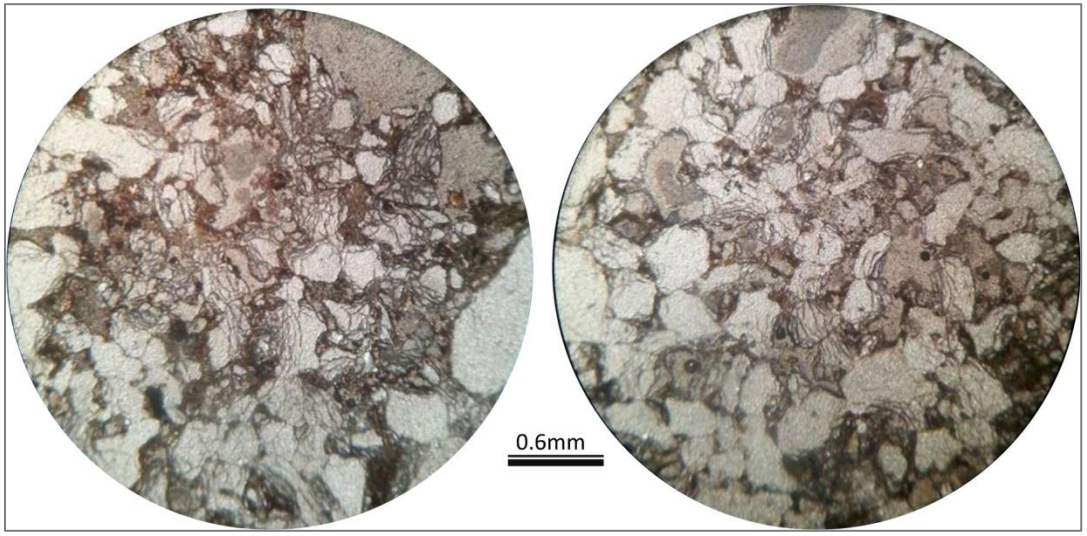

Figure 14c. Sample 2 Point-a-Pierre Formation sandstone oil impregnated.

Figure 15. Cunapo Formation conglomeratic beds at Lower Manzanilla, east coast Trinidad.

Figure 16. Electric log cross-sections along AO4 Anticline.

Figure 16a. Outcrop cross-section along OAS Quarry, M2 Ring Road, La-Fortune, Woodland, Trinidad.

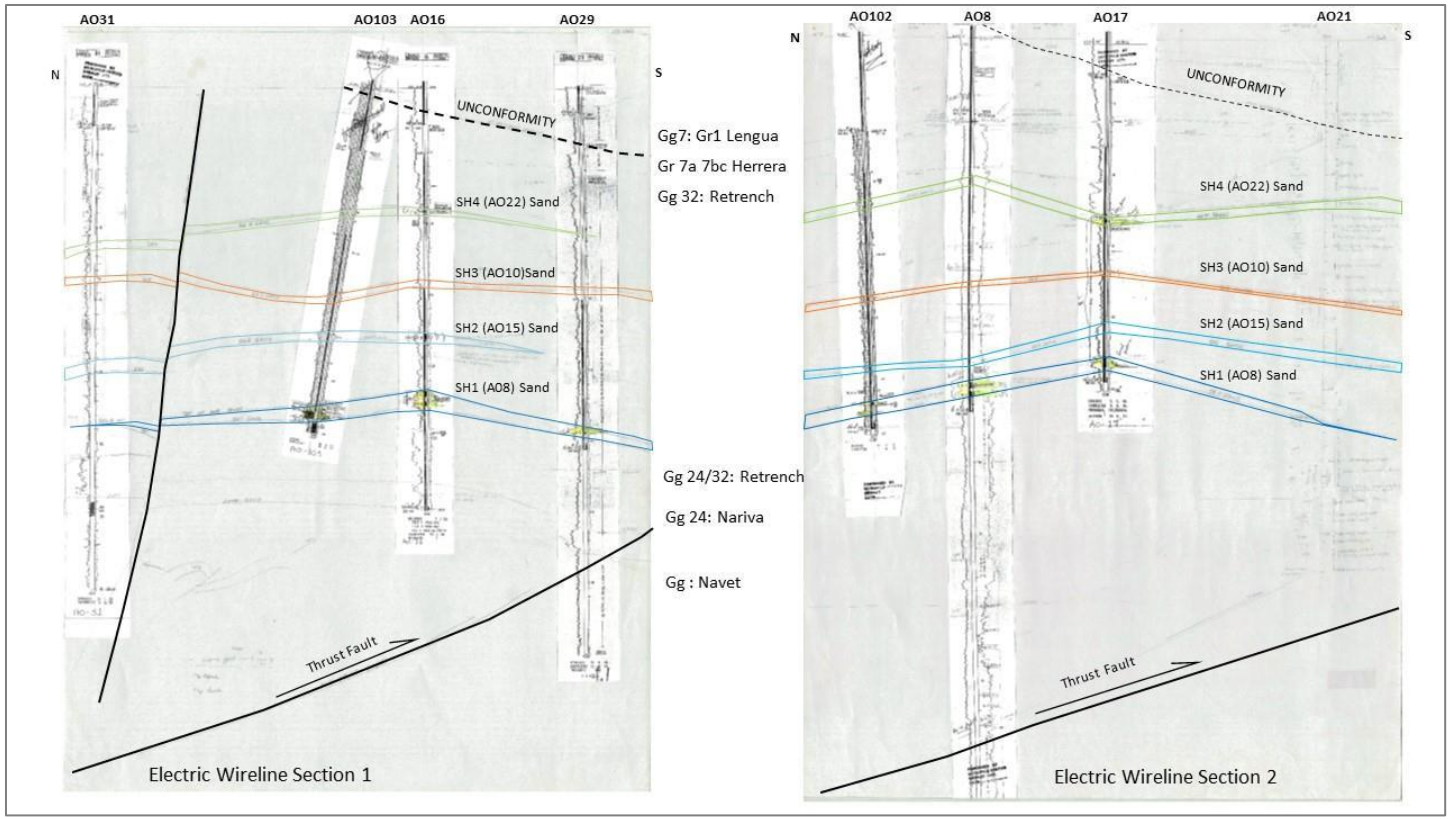

Figure 16b. Electric log cross-sections along AO4.

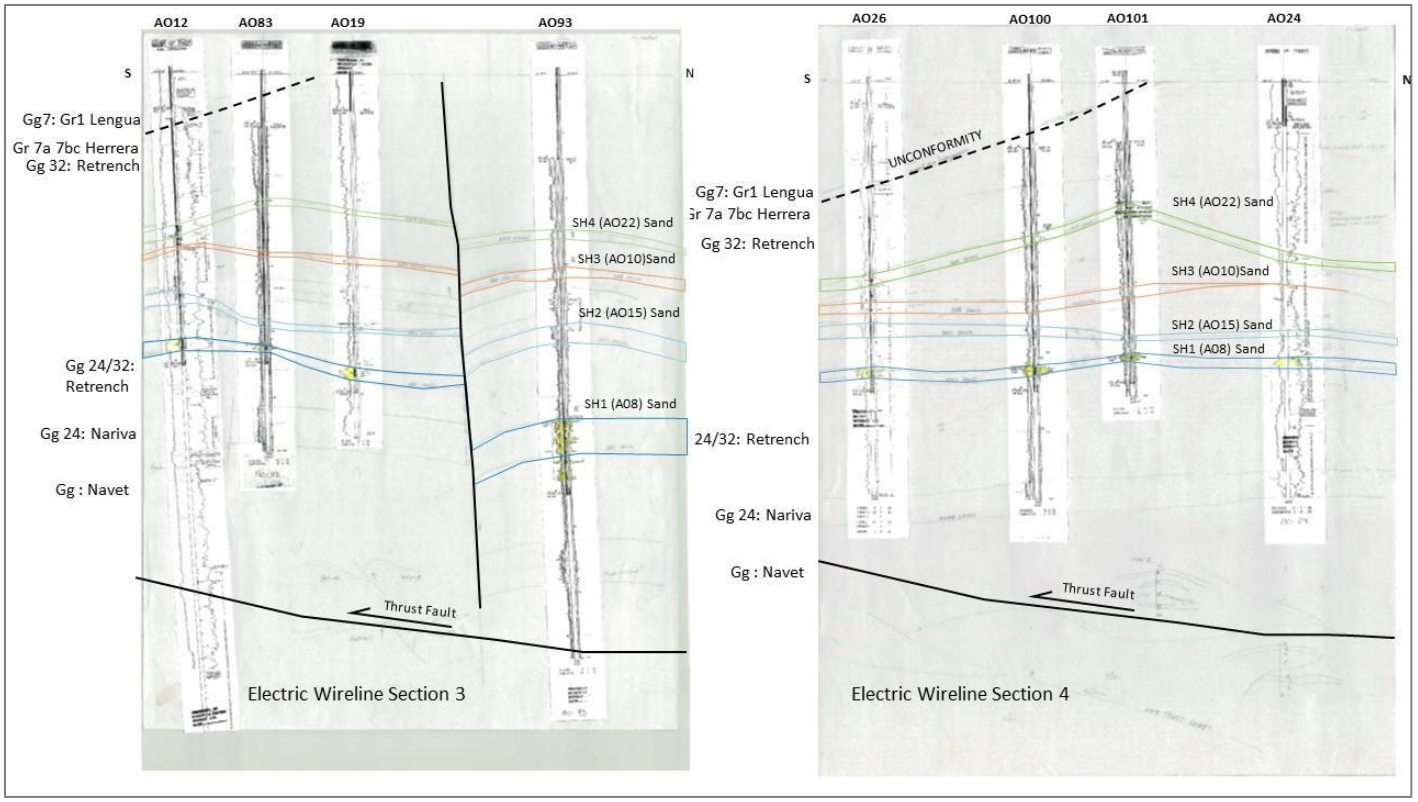

Figure 16c. Electric log cross-sections along AO4.

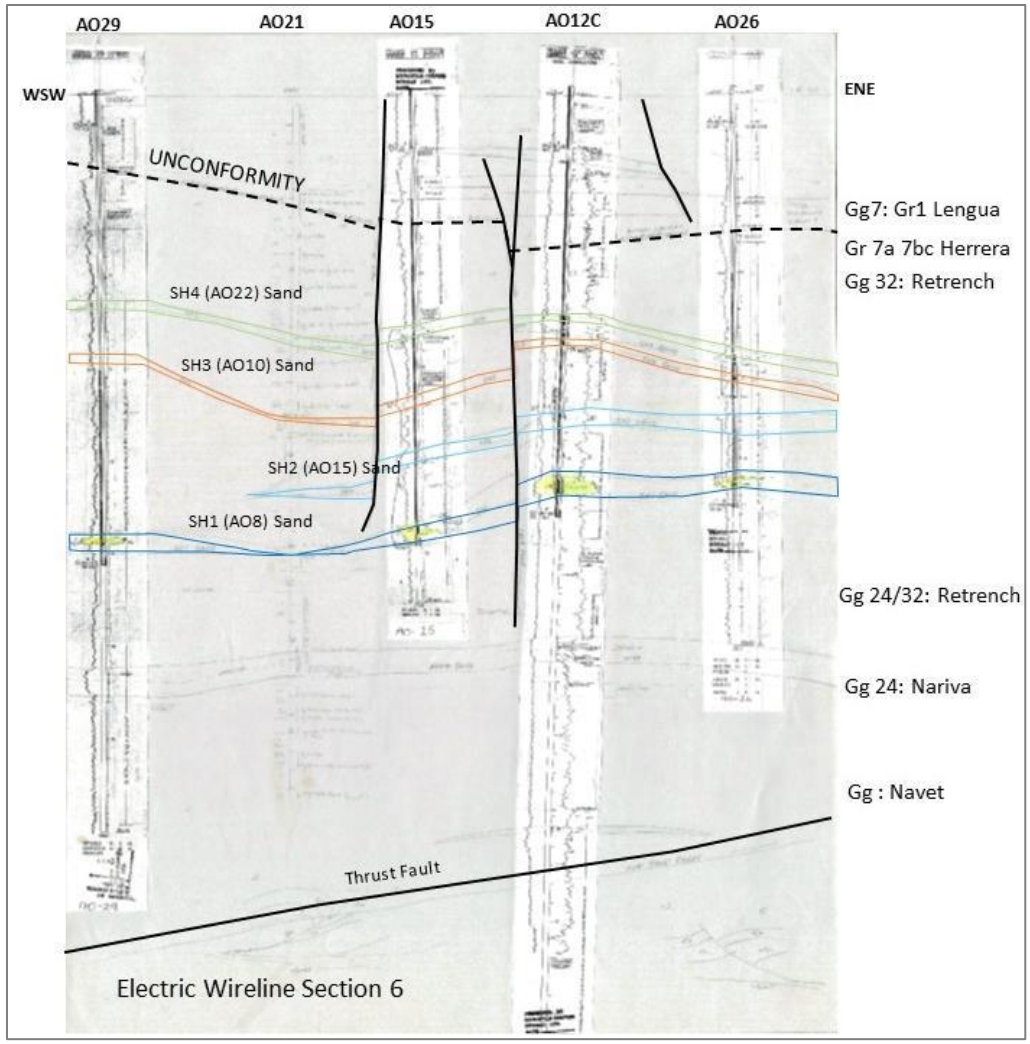

Figure 16d. Electric log cross-sections along AO4.

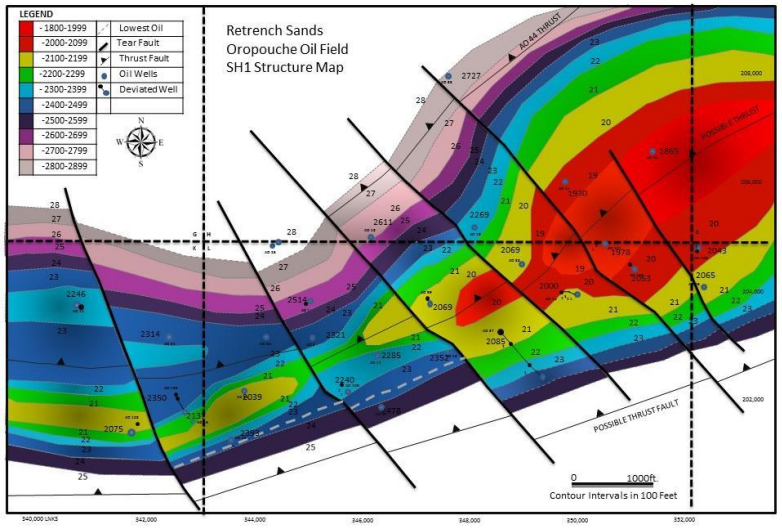

Figure 17a. SH1 structure map (top) manually constructed using Microsoft PowerPoint.

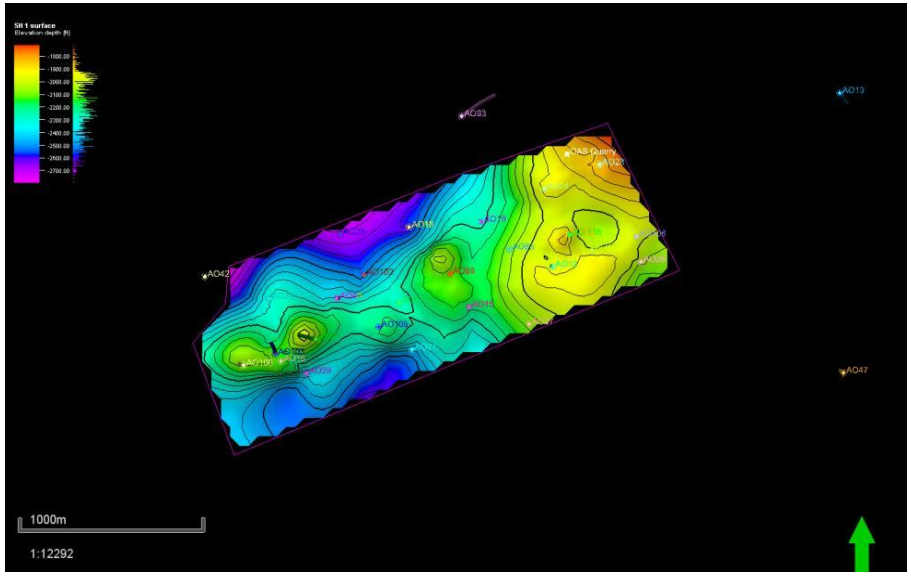

Figure 17b. SH1 Structure map using PETREL.

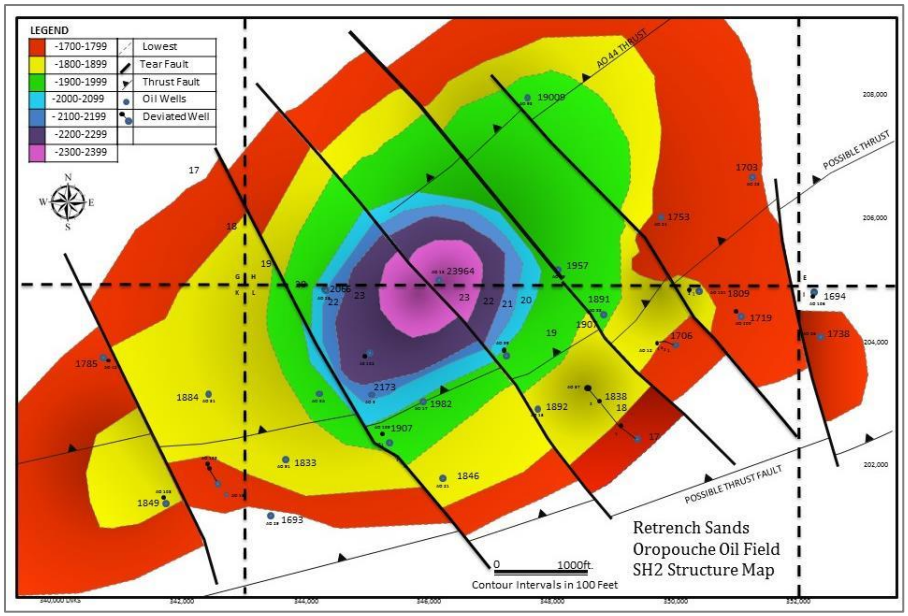

Figure 18a. SH2 Structure map (top) manually using Microsoft PowerPoint.

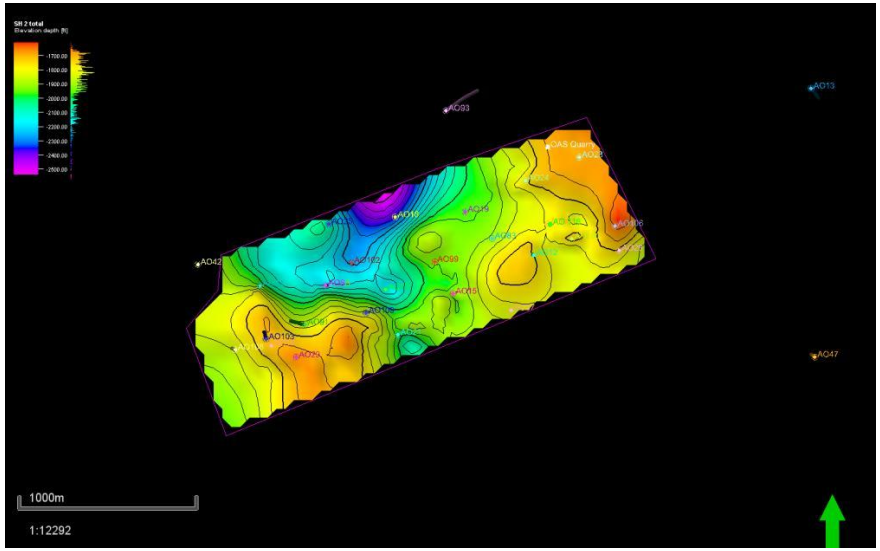

Figure 18b. SH2 Structure map (bottom) using PETREL.

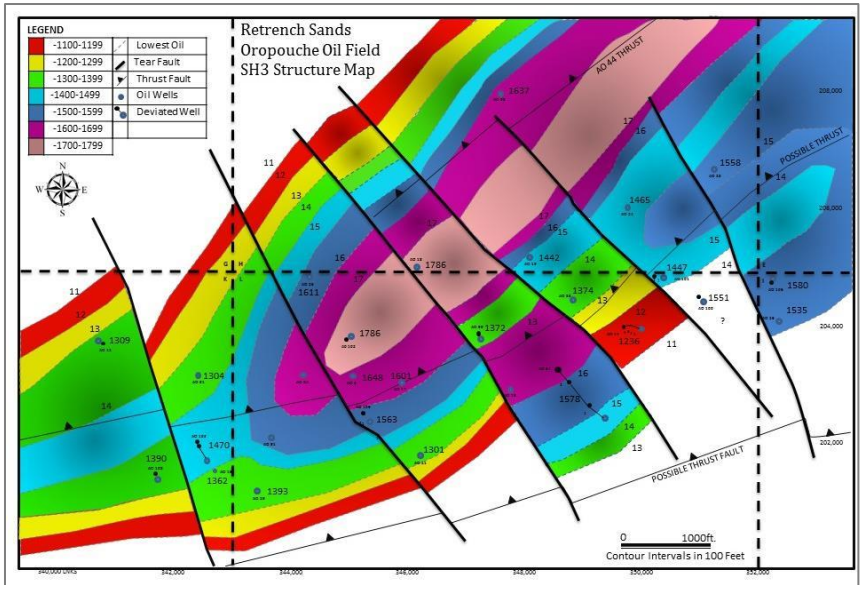

Figure 19a. SH3 Structure map (top) manually using Microsoft PowerPoint.

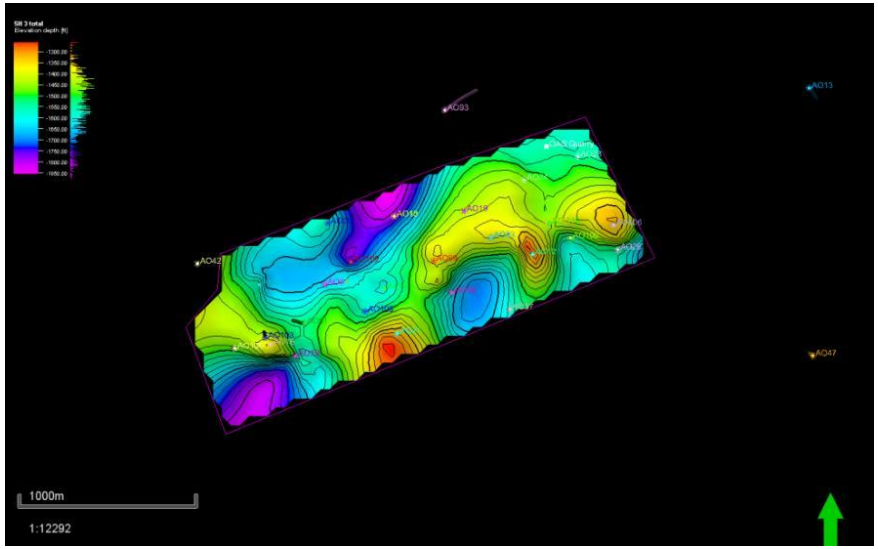

Figure 19b. SH3 Structure map (bottom) using PETREL.

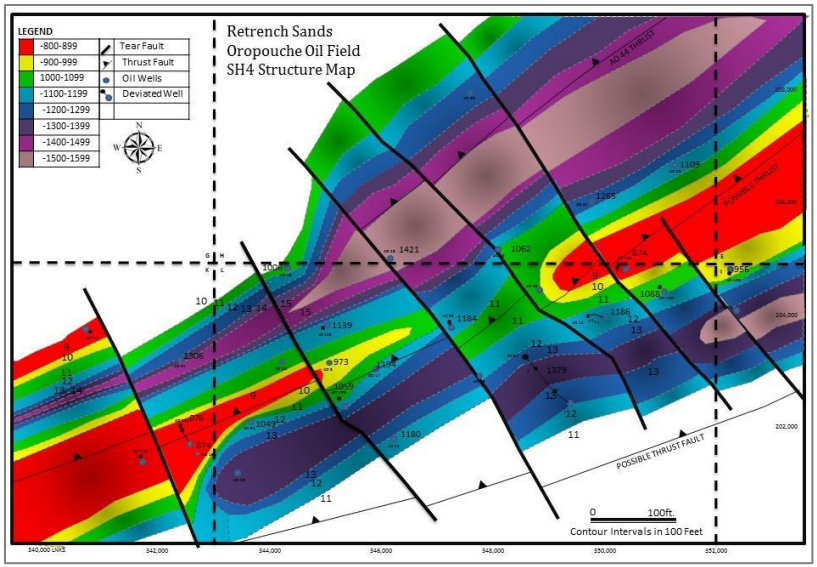

Figure 20a. SH4 Structure map (top) manually using Microsoft PowerPoint.

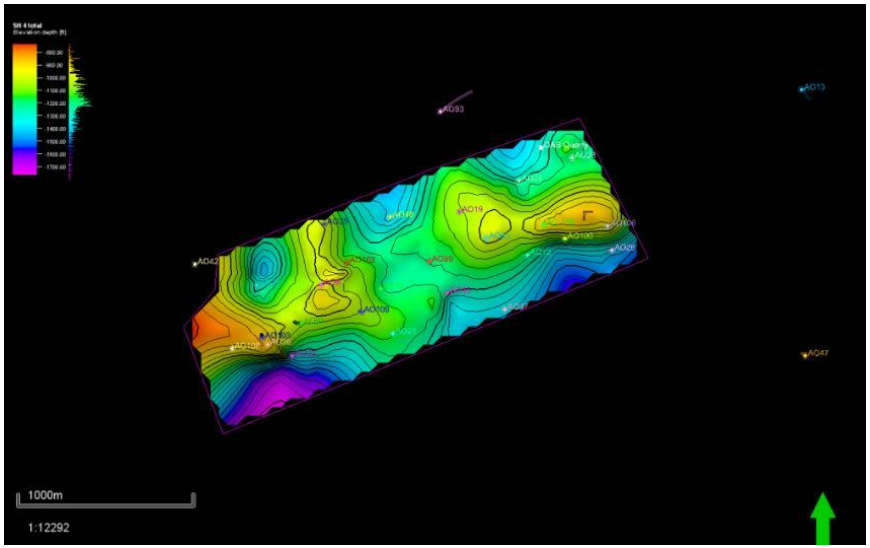

Figure 20b. SH4 Structure map (bottom) using PETREL.

Figure 21a. Golconda Interchange outcrop folding.

Figure 21b.Golconda Interchange outcrop pinchout.

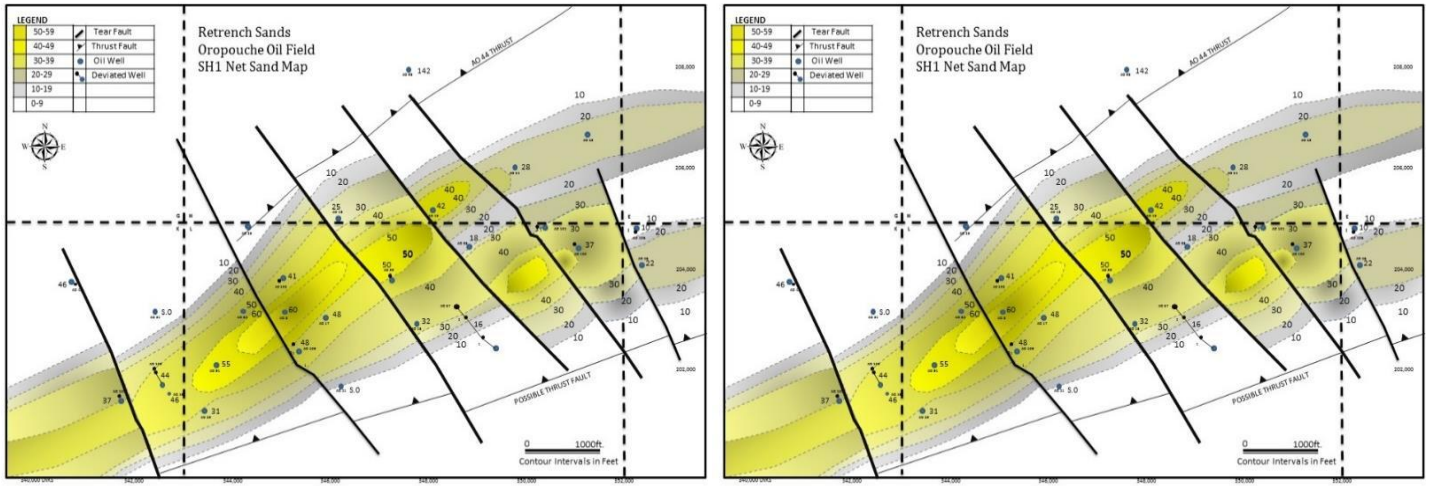

Figure 22. SH1 net sand and net pay maps.

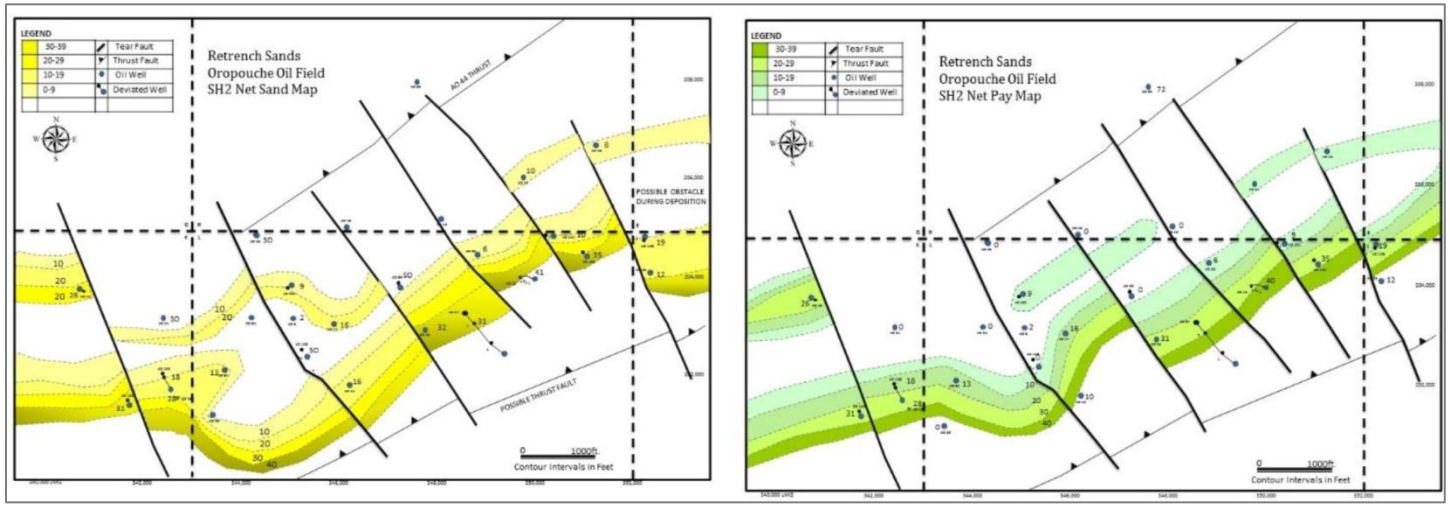

Figure 23. SH2 net sand and net pay maps.

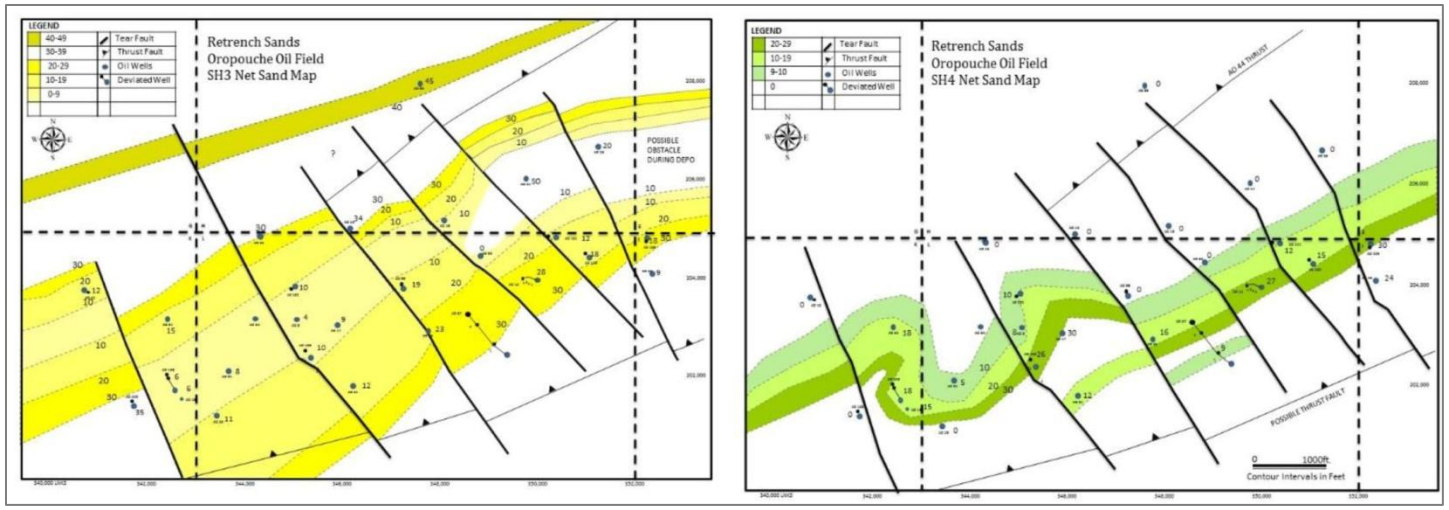

Figure 24. SH3 net sand and net pay maps.

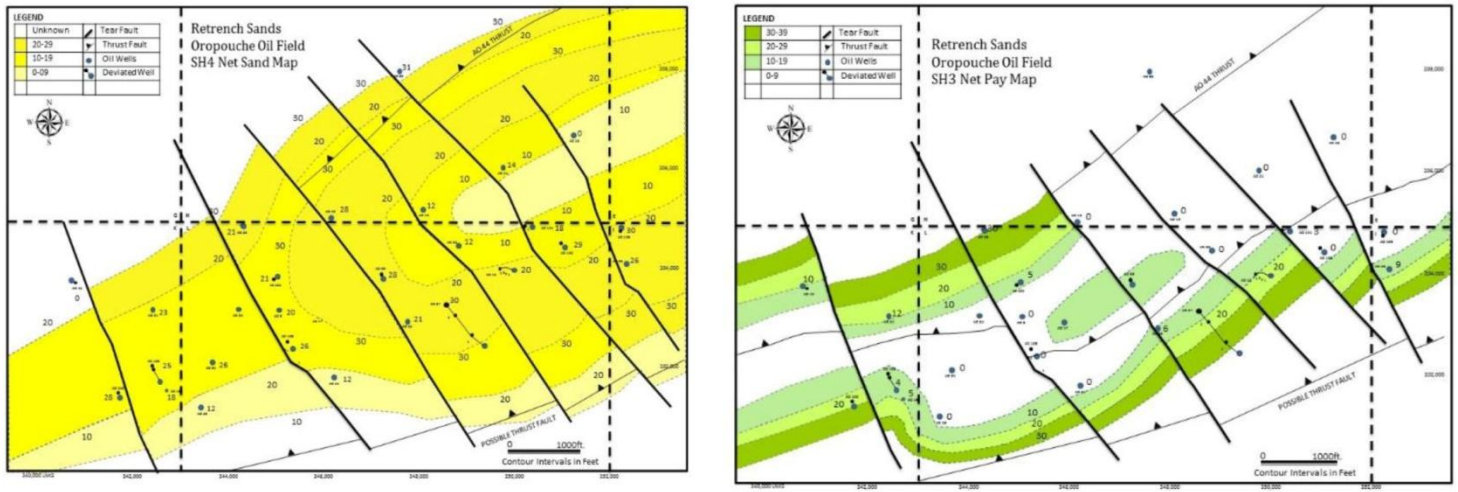

Figure 25. SH4 net sand and net pay maps.

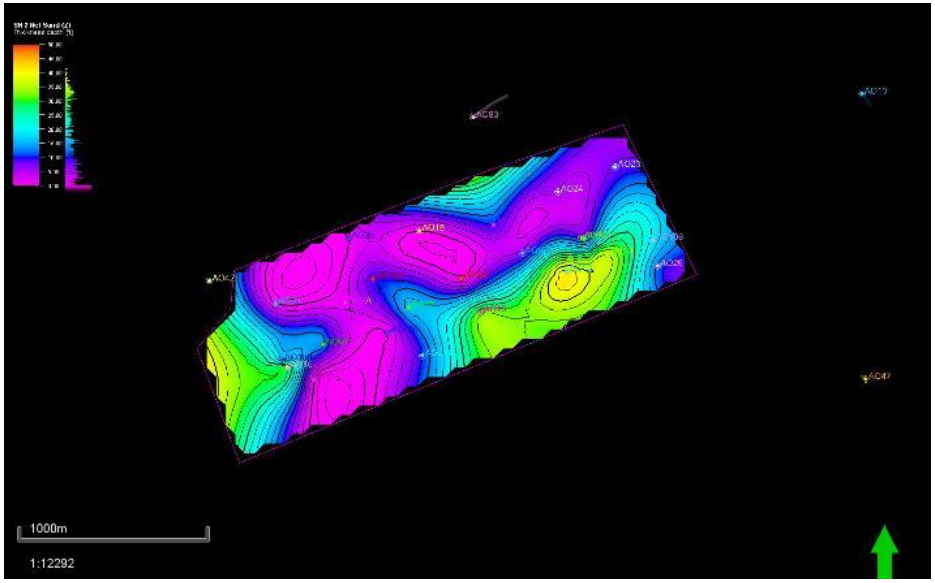

Figure 26. SH2 net sand map.

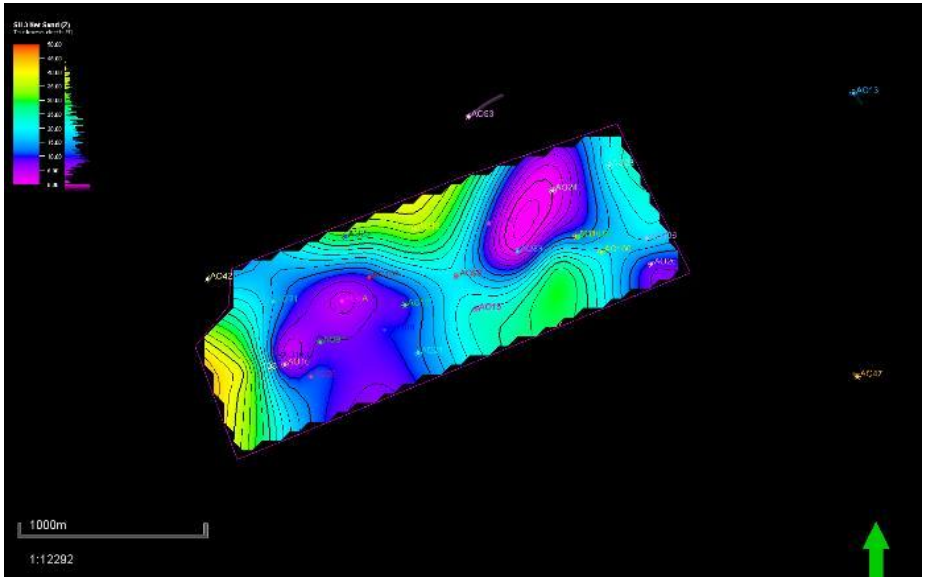

Figure 27. SH3 net sand map.

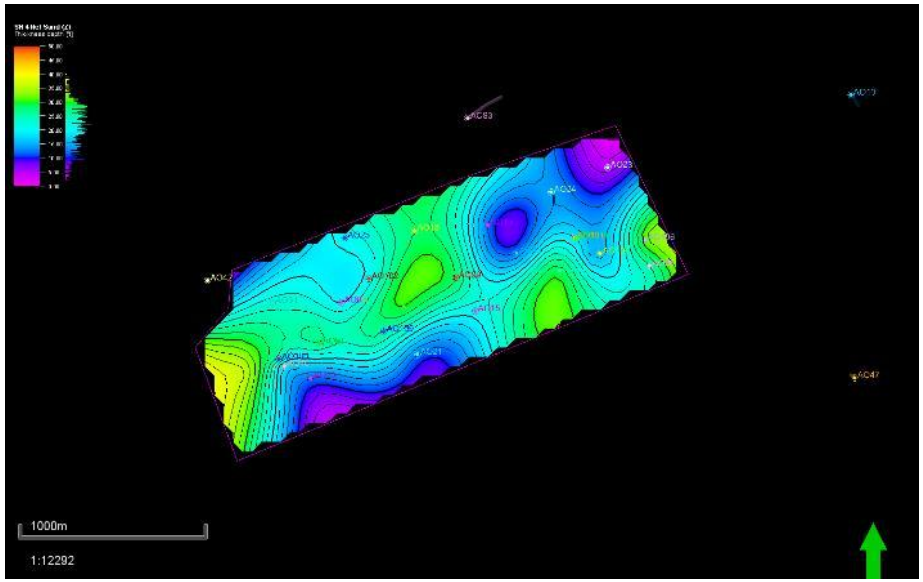

Figure 28. SH4 net sand map.

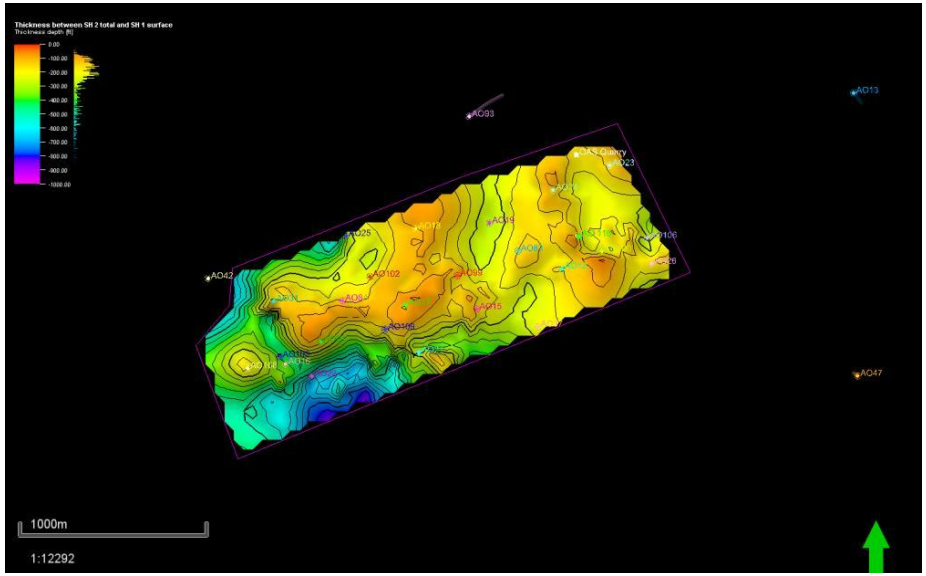

Figure 29. SH1 paleobathymetry map.

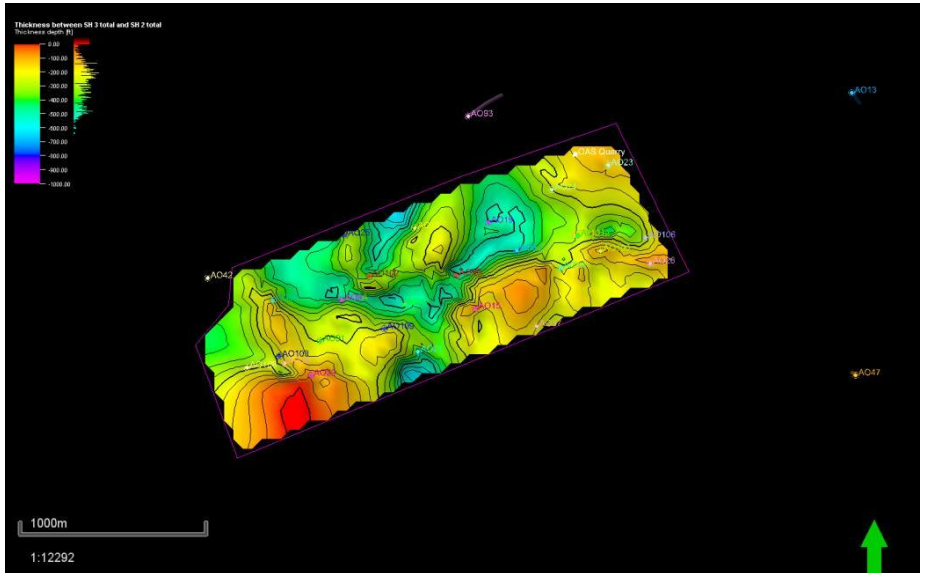

Figure 30. SH2 paleobathymetry map.

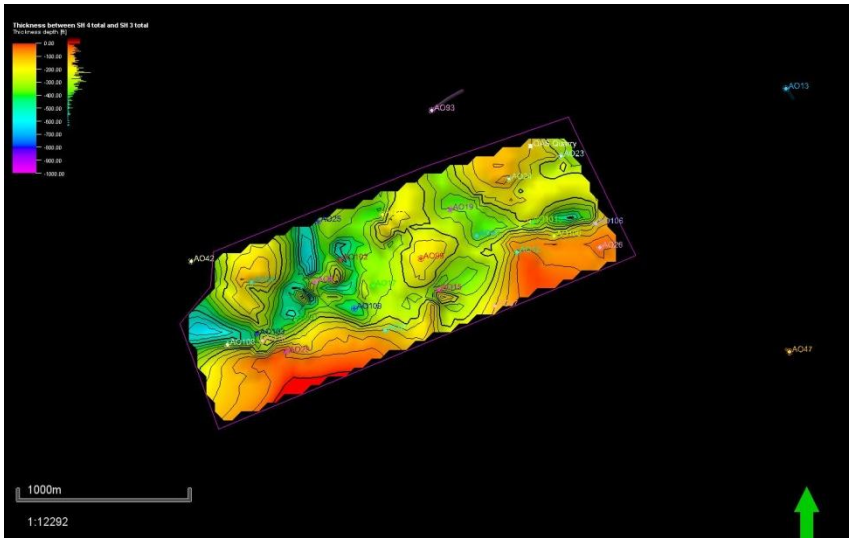

Figure 31. SH3 paleobathymetry map.

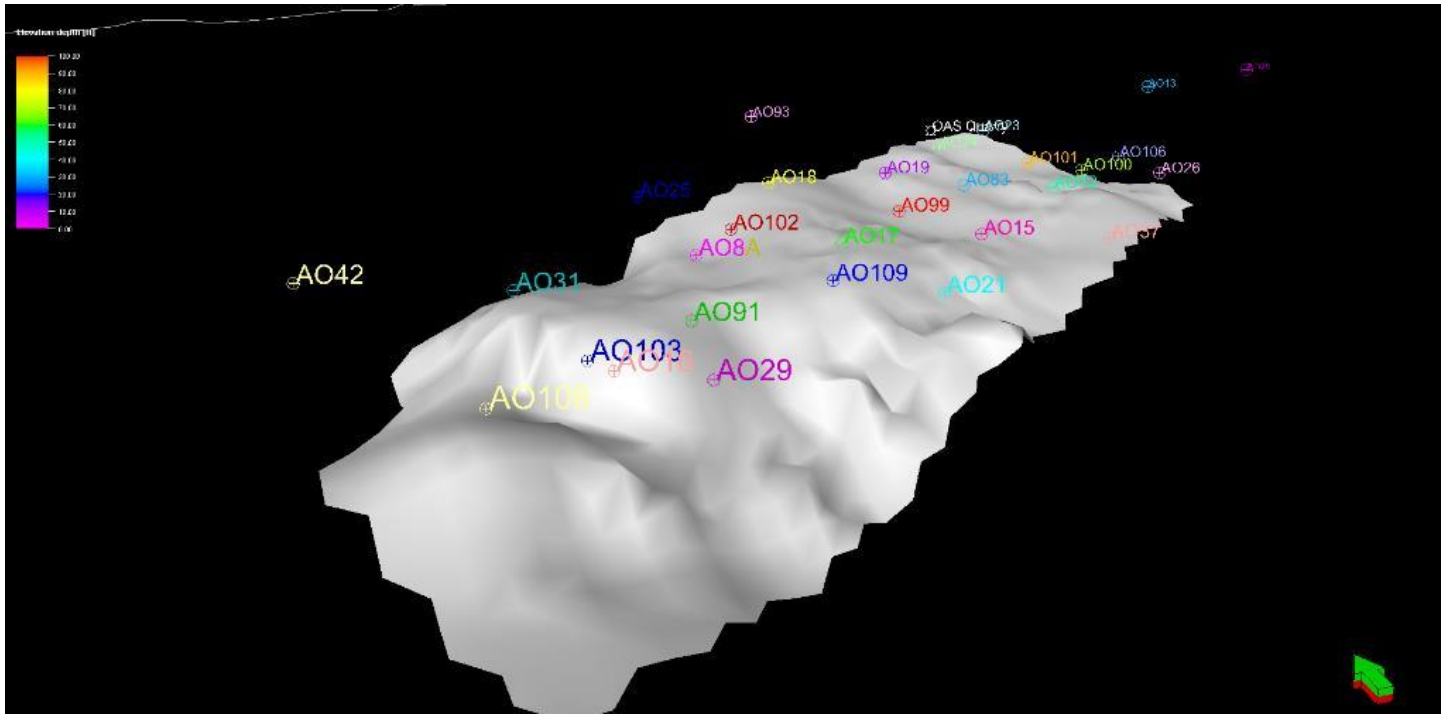

Figure 32. SH1 paleobathymetry 3D map.

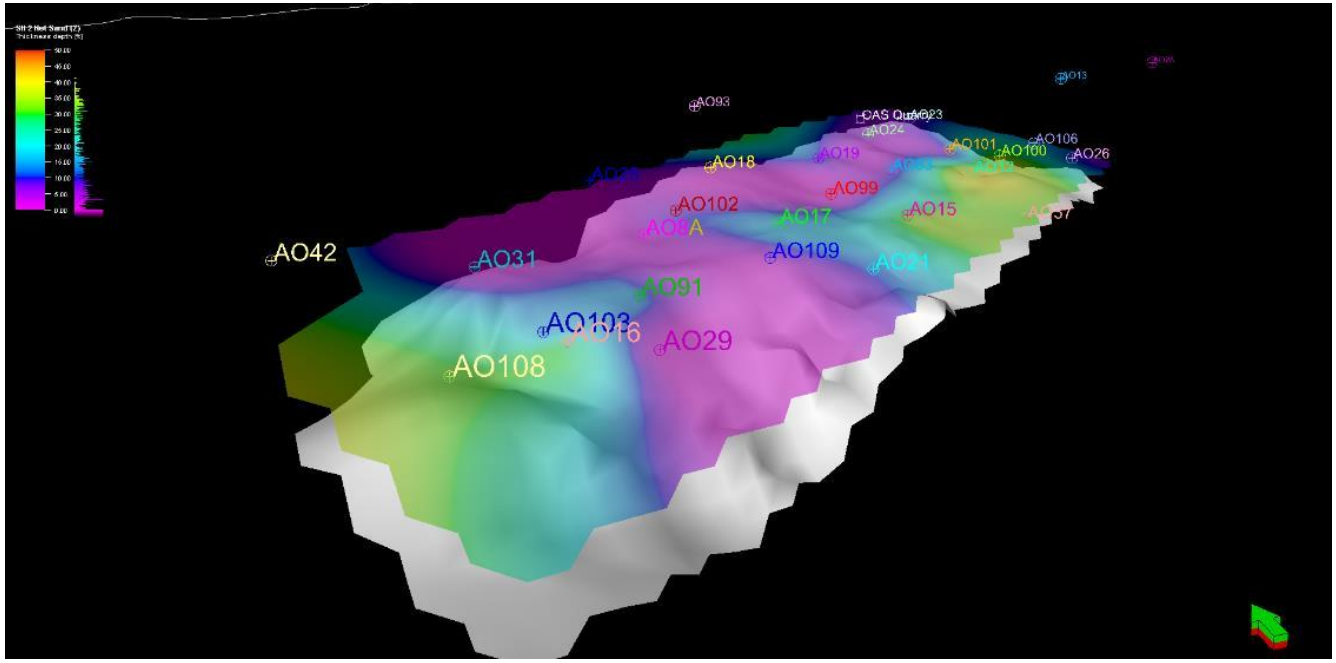

Figure 33. SH1 paleobathymetry 3D map overlain by SH2 net sand map.

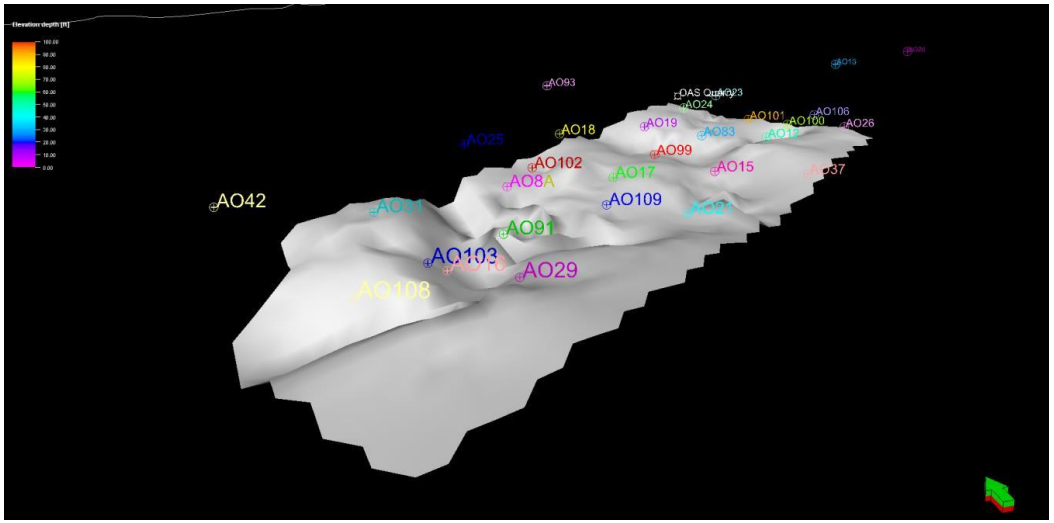

Figure 34. SH3 paleobathymetry map.

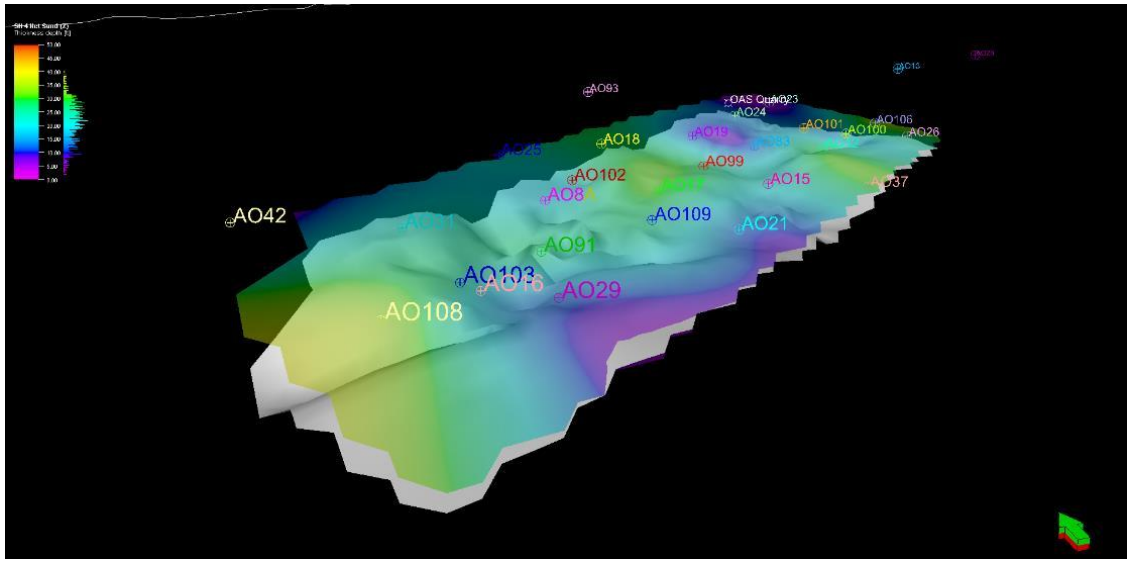

Figure 35. SH3 paleobathymetry map overlain by SH2 net sand map.

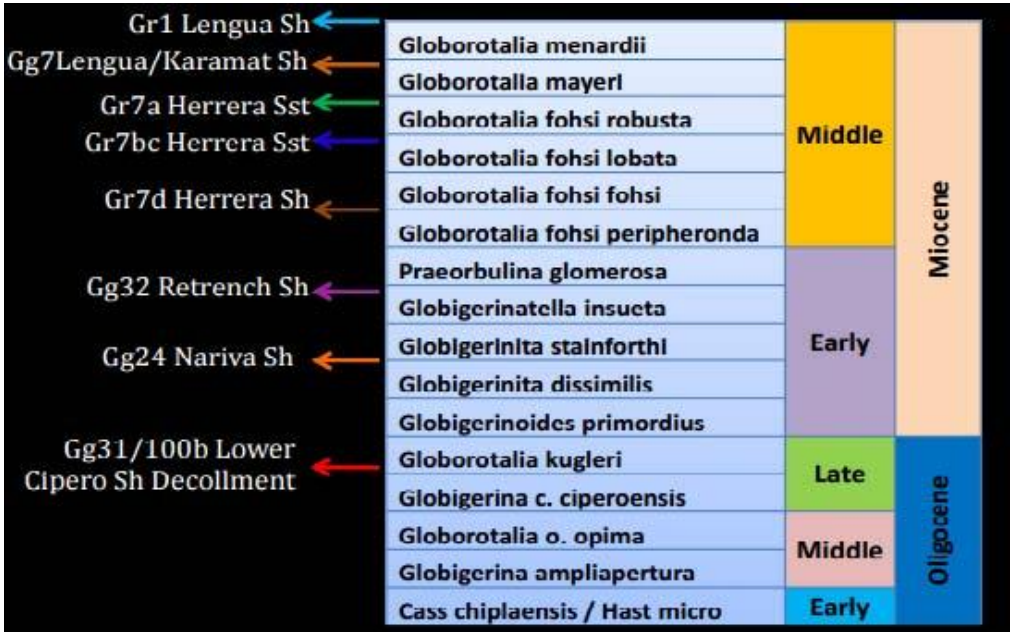

Figure 36. Partial stratigraphic chart of Trinidad from Saunders 1974 (as cited in Moonan, 2011).

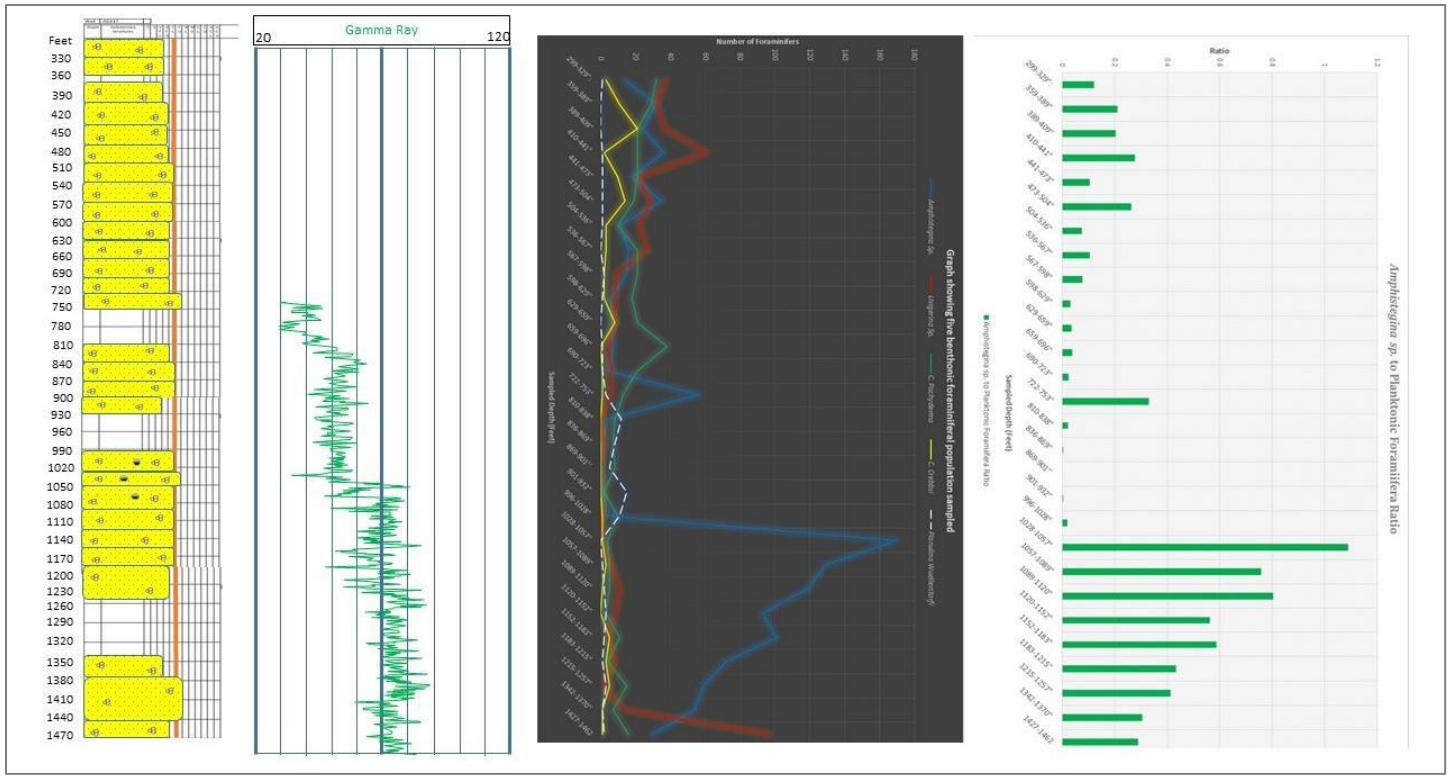

Figure 37. Comparison of litholog, gamma ray log, benthonic foraminiferal assemblage and planktonic to *Amphistegina sp.* ratio for A0117.

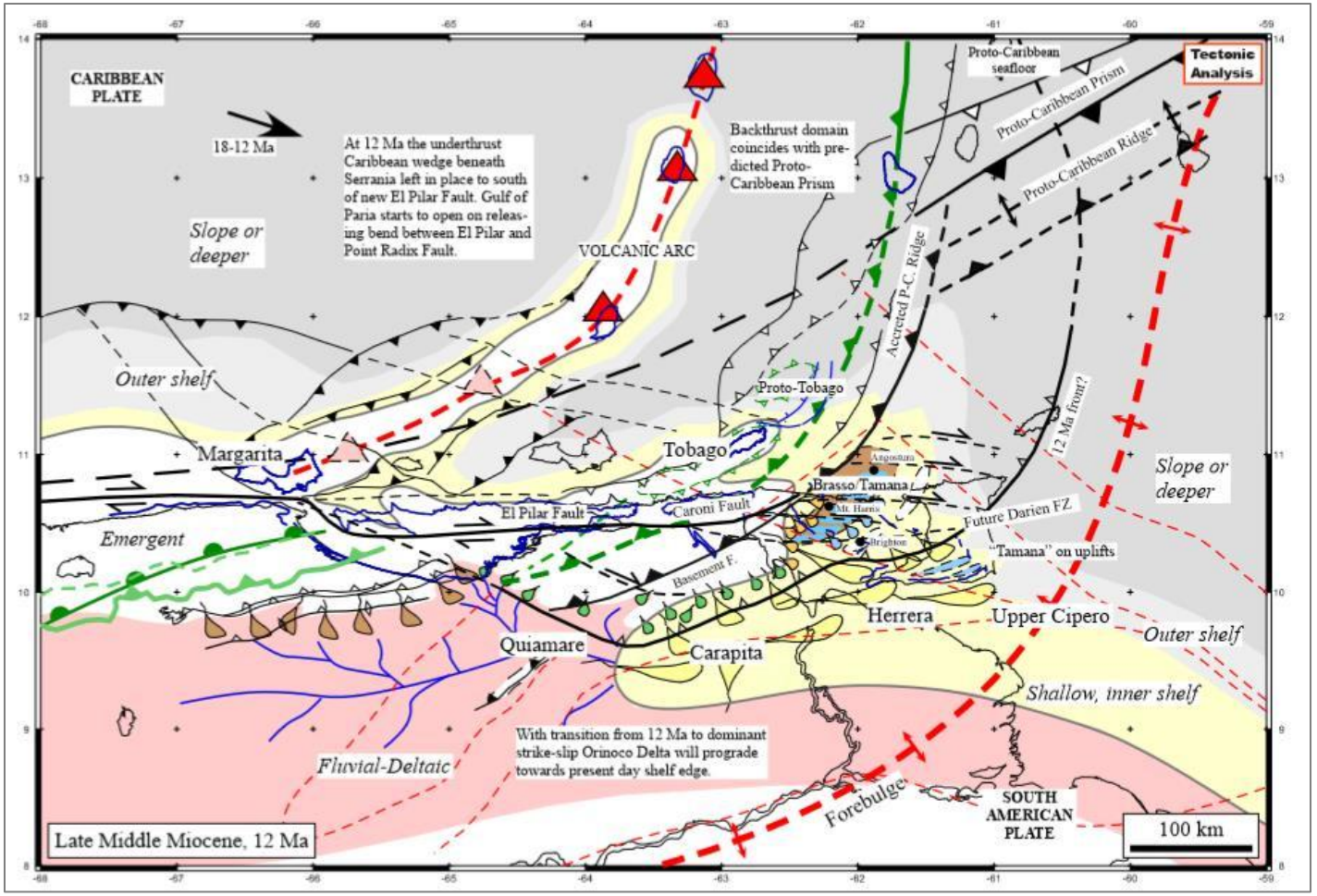

Figure 38. Late-Middle Miocene reconstruction (Pindell and Kennan, 2007).

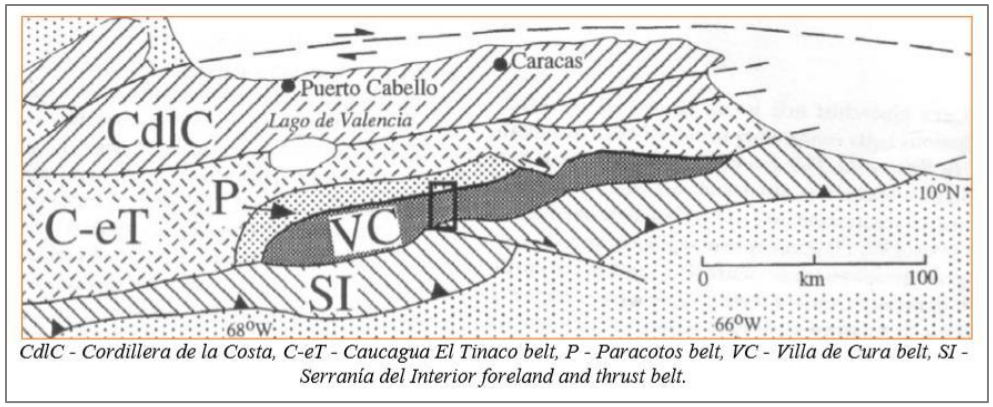

Figure 39. Simplified diagram of the Villa de Cura terrane, eastern Venezuela. Smith et al., 1999 (as cited in Urbani et al., 2005).

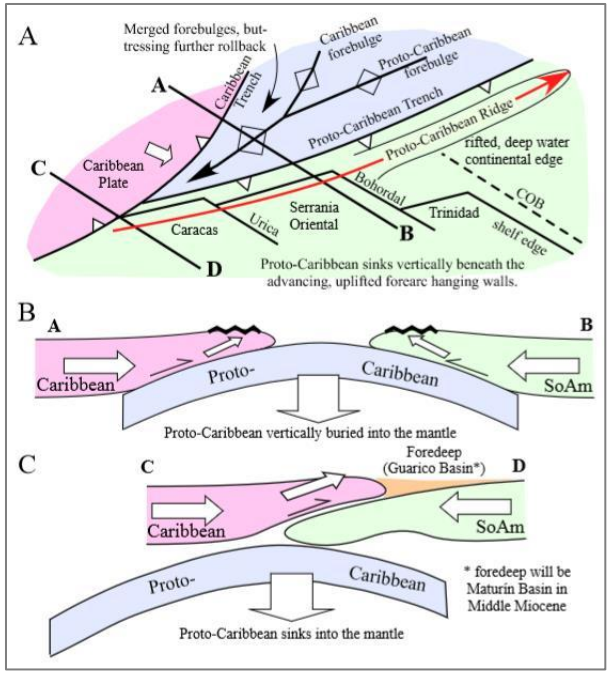

Figure 40. South American and Caribbean forebulges (Pindell and Kennan, 2007).

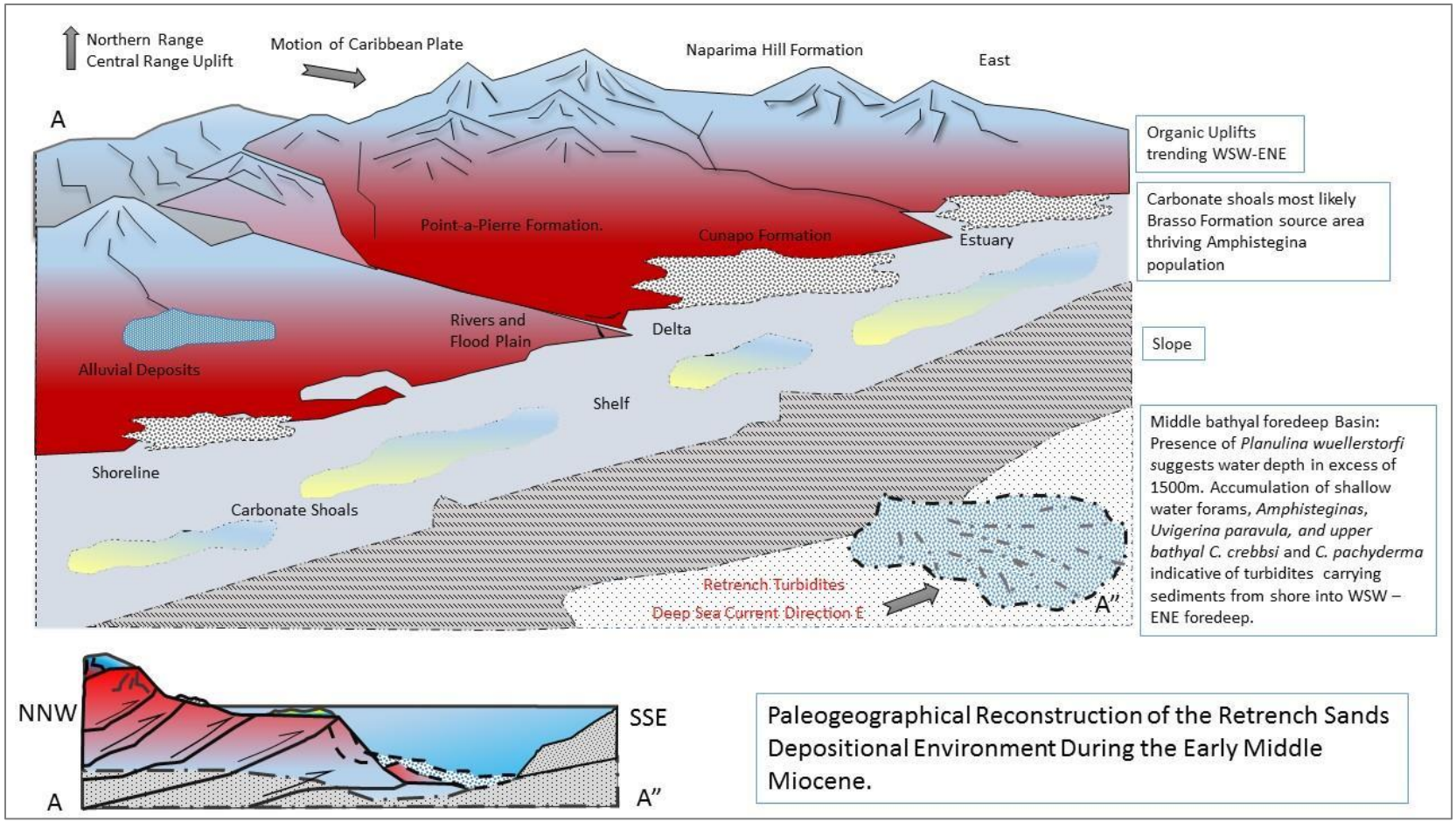

Figure 41. An uplifted Central Range where exposed Chaudière and Pointe-a-Pierre formations were the main source of quartz observed in the Retrench and potentially Herrera fairways. The quartz-rich formations could have been a result of imbrication of these arenites and possibly the Nariva Formation before it was deposited into the WSW-ENE trending, SE migrating fairways. Early thrust faulting and Central Range orogeny would have provided the mechanisms for grinding up these intensely deformed grains which continued after burial due to migrating en echelon imbricate stacks to the south/southeast with new complex anastomosing fault networks also creating a deformation apparatus. Cherts were sourced from the uplifted, sub-aerially exposed Cretaceous Naparima Hill Formation which was thereafter eroded to form the Cunapo Formation which was then subsequently eroded by rivers, sand grain abrasion during arid periods and nearshore currents which winnowed away the finer detritus into the deeper basins. Quartz and chert were then carried over the shelf edge by prograding deltas during tectonic dominated uplift in the Central Range and eustatic sea level regressions in Early-Middle Miocene thus entraining and encasing shallow water, fore-reef *Amphistegina* sp. (related to the Brasso Fm.), outer-neritic *Uvigerina paravula*, outer neritic-upper-bathyal *C. pachyderma* and upper neritic *C. crebbsi* into a middle-bathyal basin approximately 1500 m deep as suggested by the presence of *Planulina wuellerstorfi*. Shelf edge olistostrome and nearshore currents could have also contributed to turbidite input into the foredeep.